Trading off dissimilar stakeholder interests

Changing the bed level of the main shipping channel of the Rhine-Meuse Delta while considering freshwater availability

Bakker, Floor P.; Hendrickx, Gijs G.; Keyzer, Lennart M.; Iglesias, Sebastian R.; Aarninkhof, Stefan G.J.; van Koningsveld, Mark

DOI
10.1016/j.envc.2025.101323

Publication date
2025

Document Version
Final published version

Published in
Environmental Challenges

Environmental Challenges 21 (2025) 101323

Contents lists available at ScienceDirect

Environmental Challenges

journal homepage: www.elsevier.com/locate/envc

Trading off dissimilar stakeholder interests: Changing the bed level of the main shipping channel of the Rhine-Meuse Delta while considering freshwater availability

Floor P. Bakker [a,*], Gijs G. Hendrickx [a], Lennart M. Keyzer [b], Sebastian R. Iglesias [c], Stefan G.J. Aarninkhof [a], Mark van Koningsveld [a,c]

[a] Delft University of Technology, Faculty of Civil Engineering and Geosciences, P.O. Box 5048, 2600 GA Delft, The Netherlands
[b] Port of Rotterdam, P.O. Box 6622, 3072 AP Rotterdam, The Netherlands
[c] Van Oord Dredging and Marine Contractors B.V., P.O. Box 8574, 3009 AN Rotterdam, The Netherlands

ARTICLE INFO

Keywords:
Salt intrusion
Freshwater availability
Port accessibility
Estuary
Trade-off
Decision-making

ABSTRACT

Climate change and socioeconomic developments have led to highly stressed estuarine systems in which dissimilar and conflicting stakeholder interests can no longer be satisfied simultaneously, inevitably resulting in trade-offs. Since translating these stakeholder interests into quantifiable performance indicators is challenging, policy and decision-makers are often bound to qualitative trade-off assessments, potentially resulting in suboptimal system interventions. In this paper, we assess the well-known socioeconomic trade-off in estuaries worldwide: port accessibility versus freshwater availability. We consider the severely dry year of 2022 in the Rhine-Meuse Delta, for which we assess the effects of bed level change. To quantify the trade-off, we apply a general framework of performance indicators determined based on models that use the output of a validated hydrodynamic model, including salt transport. Port accessibility was quantified based on vessel waiting times, using a data-driven nautical traffic model. For the performance indicator of freshwater availability, we developed a metric that includes storage capacity. The method resulted in a trade-off curve showing improved freshwater availability and deteriorated port accessibility for decreasing bed level. This trade-off curve provides valuable insights into system interventions in a multidisciplinary setting, being an intuitive visualisation showcasing the (non-monetary) benefits and costs for different stakeholders with dissimilar interests. As the method could be expanded and applied further, this study aids quantitative policy and decision-making.

1. Introduction

Globally, deltas have been attractors of human activity and other forms of life alike. This is because they provide fertile soils and access to freshwater, as well as an open connection to the sea (Maul and Duedall, 2019; Pont et al., 2002). In addition, estuaries are also ecologically valuable systems due to their high biodiversity (Tangelder et al., 2017), and their calm waters function as nurseries (Breine et al., 2011; Tulp et al., 2008).

With their attractiveness, estuaries house many different stakeholders with often conflicting interests: (1) communities require fresh surface waters for drinking water, agriculture, and industry, and low water levels for safety (e.g., Temmerman et al., 2013; Wada et al., 2011); (2) ports demand sufficient water depths and low current velocities to facilitate safe operations for deep-draughted vessels (van Koningsveld et al., 2023); and (3) ecological diversity facilitates estuarine resilience (e.g., Folke et al., 2002; Loreau et al., 2003), which arises from a multitude of gradients generally present in natural estuaries (e.g., Mestdagh et al., 2020; Tangelder et al., 2017; Ysebaert et al., 2003).

Over time, humans have interfered in the estuarine system to optimise performances considered important: e.g., (1) channel deepening to improve the accessibility of the port (e.g., Best, 2019; Johnson et al., 1987); (2) closing off of estuaries for water safety (e.g., Figueroa et al., 2022; Orton et al., 2023); and (3) the creation of freshwater buffers for freshwater availability (e.g., Morris, 2013; Tönis et al., 2002). However, such large-scale interventions generally have negative side-effects for other estuarine functions not considered in the assessments (e.g., de Vet et al., 2017; van Wesenbeeck et al., 2014; Yang et al., 2010).

With the ongoing urbanisation of estuaries and worldwide globalisation (Maul and Duedall, 2019), conflicting stakeholder interests are becoming more stringent. Simultaneously, the changing climate

* Corresponding author.
E-mail address: F.P.Bakker@tudelft.nl (F.P. Bakker).

https://doi.org/10.1016/j.envc.2025.101323
Received 14 September 2024; Received in revised form 9 September 2025; Accepted 23 September 2025
Available online 8 October 2025

Acronyms

AIS	Automatic Identification System
KPI	Key Performance Indicator
MBL	Maintained Bed Level
NWW	Nieuwe Waterweg
PoR	Port of Rotterdam
RMD	Rhine-Meuse Delta

stresses the estuarine functions supporting these interests; e.g., resulting in reduced freshwater availability (Alcamo et al., 2007; Distefano and Kelly, 2017; Kumar et al., 2013). As a result, policies and decisions must be made regarding more sensitive trade-offs in a crowded, high-stakes environment.

Often regarded as a most influential trade-off within the conflicting stakeholder interests in the delta is the increasing demand for deeper waterways to improve port performance (Almaz and Altiok, 2012), given the increasing demand for freshwater (Distefano and Kelly, 2017; Vörösmarty et al., 2000). Deeper estuaries are, however, known to cause more salt intrusion (e.g., Hansen and Rattray Jr., 1965; Veerapaga et al., 2020; Hendrickx et al., 2023b), stressing freshwater availability. Worldwide, the economic advantages of port expansions push channels to be deepened to facilitate further port development and growth; e.g., Bahía Blanca, Argentina (Zilio et al., 2013); Hudson River, NY, USA (Ralston and Geyer, 2019); Mekong Delta, Vietnam (Nguyen and Le, 2023); Mississippi River, LA, USA (Johnson et al., 1987); Niger Delta, Nigeria (Dada et al., 2016); Pearl River, China (Yuan and Zhu, 2015); Rhine-Meuse Delta, the Netherlands (Cox et al., 2022); Yangtze River, China (Chen et al., 2019).

During normal conditions, such deepenings generally do not strain the freshwater availability. However, it is during droughts that the deepened channels may cause freshwater shortages. Substantial efforts are made to limit the impact of such channel deepening during threatening events. For example, in the Lower Mississippi River (LA, USA), a temporary earthen sill is placed during droughts to halt the landward propagation of the salt wedge (Johnson et al., 1987; Fagerburg and Alexander, 1994; Hendrickx et al., 2024). Nevertheless, the freshwater reserves were recently severely stressed (e.g., end of 2023; Miller and Hiatt, 2024). In the RMD (the Netherlands), a costly and complex freshwater distribution network is employed to transport freshwater from upstream to downstream locations to comply with the freshwater demands during a drought in response to the deepening of the main channel (HydroLogic, 2015, 2018).

Both these examples reflect rare, extreme events for the cases of the Mississippi River (Miller and Hiatt, 2024) and the RMD (Toreti et al., 2022; Wegman et al., 2025). However rare and extreme, such severe droughts fall within a trend of increasing droughts worldwide (Zhao et al., 2024), and are projected to increase in frequency and duration (Jones et al., 2024; Lee et al., 2024). Therefore, the stresses on estuarine functions increase with climate change as well, diminishing their livability.

The clear opposing interests of stakeholders pose a challenge for policy and decision-makers. Not only are the effects of water depth on the port logistics and accessibility as well as on the up-time of water intakes both highly nonlinear, their performance metrics do not align and are not easily translated to monetary units. Moreover, decision support systems in hydraulic engineering presented in the literature—e.g., Garmendia et al. (2010), Cordier et al. (2011), Kind (2014), Kragt (2013), Pinto et al. (2013)—do not explicitly quantify trade-offs between stakeholder interests given changes to the physical system. This problem is especially evident in the context of policy and decision-making concerning ports (Pearson et al., 2016). As a result, policy and decision-makers are forced to compare apples to oranges, possibly leading to suboptimal interventions in the physical system.

Therefore, this paper showcases a newly assembled framework aimed at enabling policy and decision-makers to quantitatively assess trade-offs of conflicting and dissimilar socioeconomic stakeholder interests in estuaries. We apply this framework to a case study of the highly urbanised and intensely utilised RMD, where the depth of the main channel of the delta has recently been deepened for port accessibility, but where shallowing is meanwhile considered an option to improve freshwater availability. Therefore, we focus on assessing an objective trade-off curve between stakeholder interests affected by bed-level change. To facilitate comprehension of the decision problem and the underlying method, this research is limited to the bi-objective problem between the performances of the port and freshwater supply—two of the most influential stakeholders in the area—during the severely dry year of 2022. With this, the ultimate goal of this study is to contribute as a submodule to a broader decision-support framework—specifically, a serious game, digital twin, and integrated assessment model currently being developed by den Haan et al. (2024), Wannasin et al. (2024), and Pourteimouri et al. (2024), respectively—which collectively incorporate a more comprehensive stakeholder selection and a wider range of interests.

The paper is structured as follows. Section 2 provides a detailed overview of the trade-off in the RMD. Section 3 describes the general framework of materials and methods used to quantify the effects of a changing bed level on the interests of the port and freshwater intakes. Section 4 presents the obtained trade-off curve of the performance indicators. Sections 5 and 6 provide a discussion and our conclusions, respectively.

2. Case study: lower Rhine-Meuse delta

2.1. System description

The RMD is the delta of the confluence of the Rhine (Waal and Lek branches) and Meuse rivers (Fig. 1). The delta consists of multiple branches with five effluences, with the Nieuwe Waterweg (NWW) being the principal outlet (under average discharge conditions), having an open connection to the North Sea. The main source of freshwater to the RMD is the snowmelt- and rain-fed Rhine river with an average discharge of 2160 m^3s^{-1}, compared to the average 290 m^3s^{-1} contributed by the rain-fed Meuse river (Sperna Weiland et al., 2015).

The magnitude and division of the incoming freshwater over the branches (Fig. 1) are regulated by weirs and discharge sluices. This is based on the measured water level of the Rhine at Lobith, where the river enters the Netherlands. The multi-objective goal of this water management system is to jointly (1) guarantee water safety, (2) provide and store freshwater, (3) facilitate inland shipping, and (4) protect ecological values (Rijkswaterstaat, 2019).

The NWW is designed to convey 1500 m^3s^{-1} to limit salt intrusion. This design discharge is achieved by regulating the Haringvliet Sluices (Rijkswaterstaat, 2019), which are located at the mouth of the Haringvliet, south of the NWW (HV in Fig. 1). Together with a mean annual meso-tidal range of about 1.8 m at the mouth of the NWW, this estuary is classified as a salt wedge estuary (de Nijs et al., 2011). Under such average conditions, the salt intrusion reaches 24 km inland, near the Botlek harbour (Fig. 1a; de Nijs et al., 2009).

When the discharge in the Rhine at Lobith Q_{Lobith} drops below 1700 m^3s^{-1} (typically during summer), the design discharge of the NWW cannot be maintained, causing saline water to intrude beyond the Botlek far into the Nieuwe Maas (Fig. 1b). To convey as much freshwater as possible through the NWW in this situation, the Haringvliet Sluices remain almost entirely closed (Rijkswaterstaat, 2019). The further the discharge at Lobith drops, the more saltwater intrudes landward. Besides the hindrance to inland shipping due to the shallow upstream water depths (Vinke et al., 2022, 2024), freshwater availability becomes stressed, and especially along the northern branches of the RMD, as the brackish water reaches the mouths of the Hollandsche

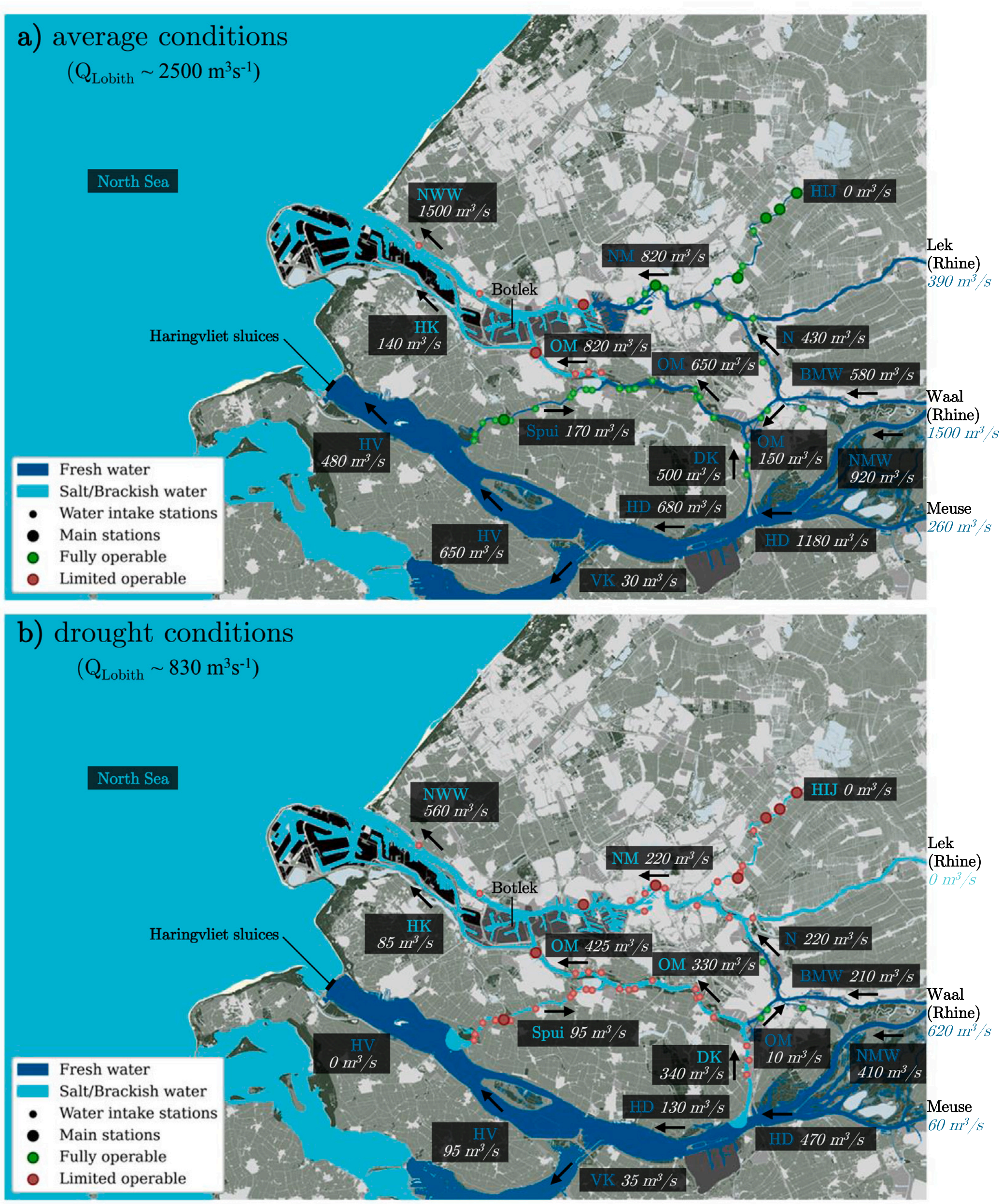

Fig. 1. Overview of the RMD highlighting its branches, including their discharge and the brackish water extent during average conditions **(a)** and during a drought **(b)**. The water intake stations that are affected by the brackish water are highlighted. **BMW**: Beneden Merwede; **DK**: Dordtsche Kil; **HD**: Hollands Diep; **HIJ**: Hollandsche IJssel; **HK**: Hartelkanaal; **HV**: Haringvliet; **N**: Noord; **NM**: Nieuwe Maas; **NMW**: Nieuwe Merwede; **NWW**: Nieuwe Waterweg; **OM**: Oude Maas; **VK**: Volkerak-Krammer. The discharges and salt intrusion, based on de Vries (2014), van der Wijk (2016),HydroLogic (2019b), are indicative and may differ from actual values due to local water extractions and flushing discharges not included in the figure.

IJssel and the Lek (Fig. 1b)—two branches with many freshwater intake stations and hardly any discharge, which is exacerbated during droughts (van den Brink et al., 2019; Wegman et al., 2025). Then, the upstream end of the Hollandsche IJssel can become fully brackish within a few days due to continuing water extractions (van Zaanen et al., 2022).

Most recently, such extreme drought events occurred in 2018 and 2022 in the RMD (Toreti et al., 2019, 2022; Wegman et al., 2025). During these droughts, the discharge at Lobith remained below 1000 m^3s^{-1}—with a minimum of 679 m^3s^{-1} in 2022—for roughly 4 and 2 consecutive months in 2018 and 2022, respectively, which caused significant damage to ecology and agriculture, and hindrance to inland shipping (Rijkswaterstaat, 2023; Vinke et al., 2022; Wegman et al., 2025).

2.2. Port of Rotterdam

Located in the RMD is the PoR, which is the largest port in Europe. It is a major stakeholder in the delta with high national and international interests. The port forms the gateway of many types of cargo and products through intermodal transport to North-Western and Central Europe. In 2022, the PoR transshipped 467.4 million tonnes of cargo (Port of Rotterdam, 2024).

The PoR can roughly be subdivided into a deepwater/offshore part, and a shallower, inland part (Fig. 1). The inland harbour basins are connected to the sea through the open connection of the NWW and Scheur, which we jointly refer to as NWW. The bed levels of the port basins and waterways are maintained by dredging according to a MBL

Fig. 2. Overview of the land-based and water-based functions in the RMD, including the design of MBL of the PoR, and the water boards (A – D) and their water intake stations (1 – 7). The asterisk ∗ marks the location of representative hydrodynamic data for water intake stations 5, 6, and 7 (upstream of the Hollandsche IJssel river). The locations of measurement data are: (i) Spijkenisse-brug, (ii) Krimpen a/d IJssel, and (iii) Kinderdijk.

design (Fig. 2). This design allows the deepest-draught vessels to reach their assigned berths.

In the port, vessels rely on tidal restrictions depending on their characteristics, e.g., draught, length, type, and destination. Vertical tidal restrictions entail regulations for minimum under-keel clearance with respect to the MBL. These result in water level thresholds along the route of the vessels. Moreover, horizontal tidal restrictions prescribe specific current velocities along their route and set limits for exceeding them. These restrictions result in time windows of opportunity for the vessel to enter the port. These so-called tidal windows interact with congestion of port infrastructure—i.e. terminals, turning basins, waterways, and anchorage areas—leading to delays in cargo transfers (Bakker and van Koningsveld, 2023).

In 2019, the NWW has been deepened from 14.5 to 16.2 m to facilitate sea-going vessels of the New Panamax class with a maximum draught of 15.0 m. Following the NWW, the Nieuwe Maas has a MBL of 14.5 m, which decreases to 11.5 m for sea-going cruise vessels to moor at Rotterdam (near intake station 4 in Fig. 2). More details on nautical traffic dynamics in the PoR can be found in Bakker et al. (2024b).

2.3. Freshwater users

The water management in the Netherlands is regulated by water boards, of which four are located in the RMD (Fig. 2): (A) Hollandse Delta; (B) Delfland; (C) Schieland & Krimpenerwaard; and (D) Rijnland. These four water boards are responsible for approximately four million inhabitants (Unie van Waterschappen, 2022), and require freshwater to fulfil three main requirements (Klijn et al., 2012): (1) water safety, (2) water quality, and (3) water quantity, such as for irrigation.

The water boards have several water intake stations throughout the RMD, which are depicted in Fig. 2. These stations predominantly consist of pumping facilities that remove excess rainfall from the polders—low-lying areas below sea level, enclosed by dikes—to the river system, and supply the polder with freshwater from the river during drought conditions. During these droughts, freshwater demand for consumption increases, in particular for irrigation. A precipitation deficit of around 0.23 m will result in a shortage of freshwater supply for consumption. A further deficit will result in insufficient water levels and flushing capacity, which causes damage to peat dikes and wooden-pile founded structures, and leads to poor water quality and consequently hindrance and damage to crops and ecology (Klijn et al., 2012).

During severe droughts—when the brackish water reaches some of the upstream water intake stations (Fig. 1b; van der Heijden et al., 2024)—the water boards redistribute freshwater amongst themselves using pumping stations. The water boards have made extensive use of these alternative routes for the freshwater, for example, during the droughts of 2018 and 2022 (Hesen, 2021; van der Heijden et al., 2024). Operation of these systems, however, leads to structural damage to the canal system and hindrance to the internal freshwater users due to increased water levels and current velocities (HydroLogic, 2018). Improvements to the system have been realised to increase its capacity at a cost of millions of euros. This led to fewer freshwater supply problems during the 2022 drought (van der Heijden et al., 2024).

2.4. Future challenges

The freshwater availability in the RMD is expected to become further stressed due to recent climatological and socioeconomic developments. These developments include (1) reduced freshwater supply due to more frequent and severe low discharge events in the Rhine (Buitink et al., 2023; Sperna Weiland et al., 2015) and increased water usage upstream (Klijn et al., 2012); (2) increased salt intrusion due to the lower discharges in the NWW and the increased offshore water levels due to sea level rise (van Alphen et al., 2022); and (3) higher freshwater demands due to more frequent and longer droughts and increased flushing discharge requirements to combat the groundwater salt intrusion (Klijn et al., 2012).

Although the current water management solution of the alternative freshwater supply routes is claimed to be effective and robust (HydroLogic, 2019a), the system may become inadequate with these developments. Extracting more freshwater from upstream to facilitate the downstream needs, causes reversed discharges in the Hollandsche IJssel and Lek branches, which exposes them to further salinisation; a problem that arose during the droughts of 2018 and 2022 (Fig. 1b; HydroLogic, 2019b; Wegman et al., 2025). As a result, freshwater was redirected from the major rivers to flush the brackish water from these branches, including other effluences that require freshwater to suppress saltwater intrusion—i.e. the North Sea and Amsterdam-Rhine Canal (van der Baan et al., 2023)—which caused further hindrance

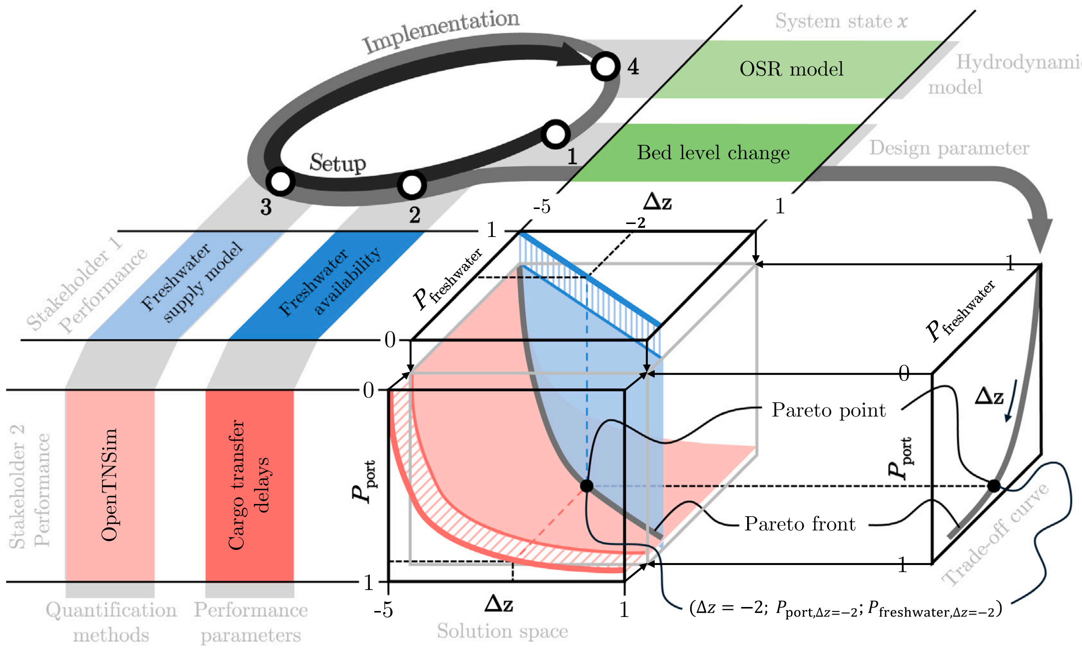

Fig. 3. The conceptual model of the trade-off method of dissimilar stakeholder interests, and its setup and implementation.

to inland shipping activities (HydroLogic, 2019b; Vinke et al., 2022, 2024). Moreover, the operation of the alternative freshwater supply system leads to costs to the water boards and their internal freshwater users (see previous subsection), and requires further extensive investments to cope with future demand, which may not be cost-effective and climate-resilient. In summary, as of the current state of the RMD, not all stakeholder interests can be satisfied. Hence, trade-offs between these interests emerge, which have to be assessed to make effective, future-proof interventions in the delta.

3. Materials and methods

To assess the impact of interventions in intensively utilised estuaries, we must quantify the implications for the affected stakeholders. Therefore, we designed a general framework that enables the trade-off of dissimilar stakeholder interests (Fig. 3). The framework is alternative-focused, i.e. focused on quantifying the trade-offs between conflicting interests of pre-identified stakeholders, given predefined alternatives. Therefore, it is not meant to facilitate identification of key stakeholders and selection of the most promising alternatives based on a value-focused stakeholder and decision analysis (Keeney, 1996). The setup of the multidisciplinary trade-off framework comprises the following four steps (Fig. 3):

1. Select a set of design parameters that captures the main properties of the alternative, given how it can affect the physical environment.
2. Determine the stakeholder interests that are directly or indirectly affected by this set of design parameters and translate these into performance indicators.
3. Define quantification methods that translate the environmental conditions to the performance indicators.
4. Select models—or a pipeline of models—that can reflect the environmental conditions based on the set of design parameters.

After the performance indicators are quantified, a trade-off method should be deployed to trade off the two stakeholder interests, for which we selected multi-objective Pareto optimisation.

The implementation of the multidisciplinary trade-off framework is in reverse order of the above implementation and consists of the following three steps (Fig. 3):

- 1 → 4: A certain system state x of the design parameter (i.e. bed level change, Δz) feeds into a hydrodynamic model (i.e. *OSR model*, see Section 3.1).
- 4 → 3: The output of the hydrodynamic model is used in quantification methods that calculate the stakeholder performance indicators (i.e. nautical traffic model OpenTNSim and freshwater supply model, see respectively Section 3.2 and Section 3.3).
- 3 → 2: The quantification methods result in the stakeholder performance indicators (i.e. cargo transshipment delays for the port, P_{port}, and freshwater availability, $P_{\mathrm{freshwater}}$, both ranging from 0 (worst) to 1 (best), see Section 3.4).

Varying the system state x of the design vessel (e.g., −5 to 1 m of bed level change, Δz) generates Pareto points for the two indicators, for example point ($\Delta z = -2$; $P_{\mathrm{port},\Delta z=-2}$; $P_{\mathrm{freshwater},\Delta z=-2}$) in Fig. 3. Together, these points form a Pareto front, i.e. the dark grey line in the square solution space. This front can be flattened to a mathematical relation between the two performance indicators, the trade-off curve.

In this study, we test the above framework to assess the impact of bed level change on the performance of the Port of Rotterdam and the water boards in the RMD. Bed level change is specifically chosen as this is a most promising parameter to reduce saltwater intrusion in estuaries (Hendrickx et al., 2023b), and is of high interest for ports due to the trend of increasing vessel dimensions and their impact on port performance (Ueda et al., 2025). We assessed the impact on the stakeholder objectives using data of year 2022.

As decision intervals related to bed level designs are typically in the order of tens of years due to the involved capital and maintenance dredging costs and underlying contracts, preferably, an equal or longer multi-year study period should be evaluated to include variability on a longer timescale (e.g., due to climate change). However, within this study, computational cost constraints did not allow for incorporating this sensitivity. The specific year 2022 was selected as it has an extremely dry summer (Toreti et al., 2022; Wegman et al., 2025), so far the driest of the 21st century and comparable to the driest on record in the Netherlands, which occurred in 1976 (Beersma et al., 2004). Therefore, it can be considered normative for the performance of freshwater supply by the water boards for the near future. Moreover, the year 2022 is also considered relevant for the Port of Rotterdam, as the traffic conditions showed no strong exceptions with other years[1], and we believe that the nautical traffic behaviour is to a lesser extent affected by climate change effects for the coming years. Nevertheless, the implications of this simplification are further discussed in Section 5.1.

We selected the MBL as the design parameter, considered as bed level change, Δz. A positive value (i.e. $\Delta z > 0$) reflects an increase in MBL—i.e. increased water depth—and vice versa. To determine the affected environmental conditions, we used a numerical model of the RMD that could determine the effects of bed level change on the local hydrodynamics (Section 3.1). Its output data was subsequently used in models that quantify the effects of changes in the hydrodynamics on cargo delays (Section 3.2) and freshwater availability (Section 3.3). At last, we translated these effects into performance indicators, which allowed for the construction of a Pareto front to provide insights into the relevant trade-off between the stakeholder interests (Section 3.4).

3.1. Hydrodynamic model and scenarios

To quantify the stakeholder interests described in Sections 3.2 and 3.3, data on water levels, flow velocities, and salinity are required throughout the RMD domain. To gather this hydrodynamic data and evaluate how it is affected by changes in the MBL, we used a coarse version of "Operationeel Stromingsmodel Rotterdam" (OSR). OSR is a deterministic, process-based hydrodynamic model that discretises the shallow water equations (derivations of the Navier–Stokes equations for incompressible free surface flow) in time and space, i.e. the RMD domain in 2022. The model uses a constant time step of several seconds and a relatively coarse three-dimensional water depth-varying computational grid with cell dimensions in the order of tens of meters horizontally (differs spatially) and ten layers over the depth, following a static, surveyed bathymetry. The model is run operationally by the PoR to provide information for the pilots, and is well-calibrated for water levels and current velocities, and also thoroughly validated for salt intrusion (Kranenburg et al., 2015).

The hydrodynamic model is used to hindcast the year 2022, for which time-varying boundary conditions for year 2022 are used, consisting of measured river discharges and modelled—from a validated larger-scale hydrodynamic model—water levels and salinities. The reference model run simulates the MBL of the NWW as the existing situation (16.2 m; $\Delta z = 0.0$ m). We validated the salinity predictions of this run against salinity measurements of the year 2022 at three locations (see Fig. 2). Although not the main objective of the model, salinity predictions are good ($R^2 = 0.9073$; Fig. 4a), where the largest errors occur at locations of higher salinity levels (Fig. 4b). With the focus on breaching a threshold value ($s_{limit} = 150$ mg Cl$^-$ l^{-1}), it is most relevant whether the model predicts the exceedance of this threshold correctly, which it does for 91.1% of the time (Fig. 4a); when incorrect, it generally underpredicts the salinity—i.e. the model overestimates freshwater availability.

Based on the PoR's accessibility policy and the distribution of draughts of vessels that navigate the NWW, we drew a total of five shallowed MBL designs ranging from 11.2 m ($\Delta z = -5.0$ m) to 15.2 m ($\Delta z = -1.0$ m), with steps of 1.0 m (see Fig. 5). Shallower MBL designs were not assessed, as these were expected to result in an unreasonably poor port performance. In addition to these runs, a scenario of a deepening of 1.0 m to a MBL of 17.2 m was assessed to show the effect of a further deepening ($\Delta z = +1.0$ m).

[1] https://www.portofrotterdam.com/en/pressroom/throughput-figures

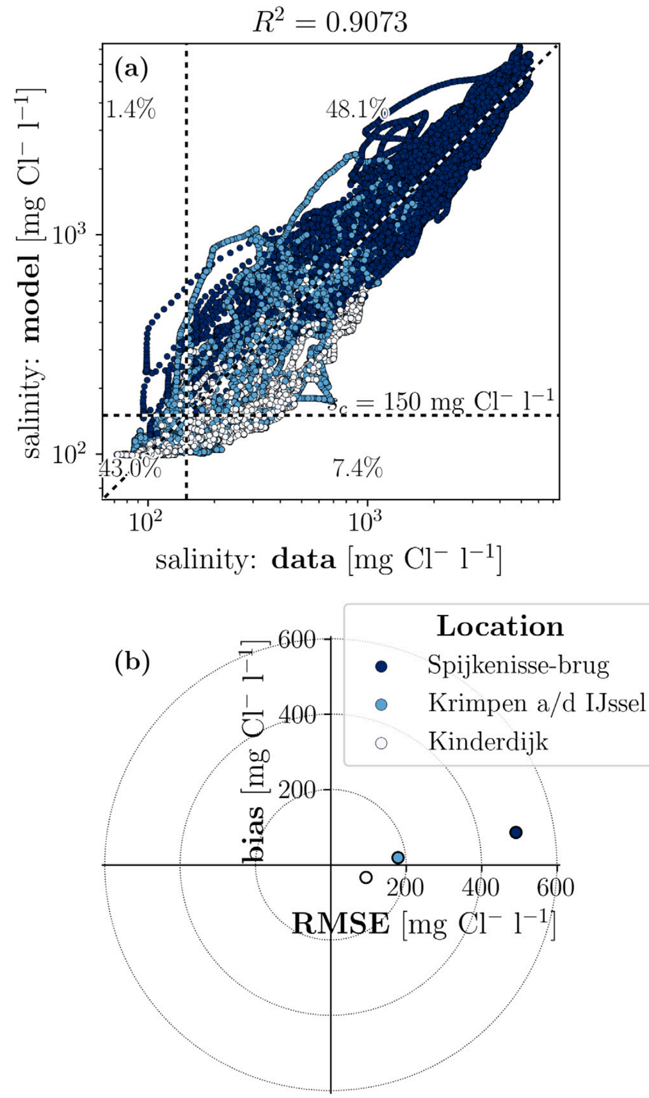

Fig. 4. Predictive power of hydrodynamic model regarding salinity. **(a)** Measurements versus predictions with the salinity threshold (s_{limit} = 150 mg Cl$^-$ l^{-1}) marked with a black, dashed line; and **(b)** target plot displaying the root-mean-squared-error (RMSE) and bias.

3.2. Quantifying cargo transshipment delays

A port relies principally on the efficient handling of its throughput. An efficient port means that cascading waiting times in cargo transshipments due to downtime and congestion of port infrastructure should be limited. Shallower MBLs can increase these waiting times, as more vessels will rely on tighter tidal windows, decreasing the port's accessibility. Moreover, shallower bed levels can decrease the throughput to the inland port, as the deepest-draughted vessels of a fleet may be unable to safely navigate to their assigned berth. If these vessels are redirected to more offshore terminals, congestion at these terminals can be expected, resulting in a further decrease in port efficiency.

To quantify the effects of bed level change on this parameter, we deployed an existing nautical traffic model for the PoR, which was presented and validated for a specific terminal in Bakker et al. (2024b). This deterministic, agent-based model, written in the open-source simulation library OpenTNSim (van Koningsveld and den Uijl, 2019; Baart et al., 2022), estimates the cascading vessel waiting times due to the interaction between tidal downtime and berth congestion for the Botlek area. For this, the model uses discrete-event time discretisation to simulate individual vessels moving over a network graph. Thereby, the model assesses vessel behaviour and subsequent waiting times by resolving interactions between vessels, capacity-limited wet port infrastructure, and hydrodynamics, using algorithms that capture the accessibility and berthing policy of the PoR.

In this study, we extended the existing model to include seagoing traffic bound to other inland sea terminals that are affected by bed level change. For this, we used four data sources from 2022: hindcasted vessel data from AIS, hydrodynamic outputs from the OSR model, geospatial data, and the port authority's tidal restriction regulations for each inland harbour basin. Based on this data, 12 terminals were selected that are affected by tidal restrictions and yearly operate at least 20 vessels that are affected by a bed level change of $\Delta z = -5.0$ m. The following inputs for the nautical traffic model were derived: (1) the location of the PoR's wet infrastructure and their properties (e.g., capacity, MBL, and tidal restrictions); (2) the vessels of call, including their properties (e.g., draught, laytimes and speed); and (3) the tidal hydrodynamics (i.e. water levels and current velocities). Details on the processing of the above data and the setup of the nautical traffic model can be found in the software publication of Bakker et al. (2024a), accompanying the earlier validation study of the nautical traffic model (Bakker et al., 2024b).

As the shallower bed levels are expected to fully restrict the passage of the deepest-draughted vessel through the NWW, the cargo throughput to the inland terminals may drop. We assume that this is not acceptable for the port, and therefore, this throughput will be maintained in the model using replacement coasters. This means that arriving vessels with excess draughts are assumed to be redirected to a feeder terminal in the offshore port. There they will be lightened and the excess cargo will be transferred to and transshipped by coasters with a total equivalent transport capacity to the inland terminal. Moreover, departing vessels with excess draughts are loaded with their excess cargo at the offshore feeder terminal. Again, this cargo is transshipped by coasters from the inland terminal.

3.3. Quantifying freshwater availability

The interest of the inhabitants of a delta—or surrounding an estuary—were reflected by freshwater availability. To assess this, we use a deterministic, process-based volume-balance method that includes freshwater supply, demand, and storage for each water board b separately (Eq. (1)):

$$\frac{\mathrm{d}V_{s,b}}{\mathrm{d}t} = E_b(t) - D_b(t) \tag{1}$$

where $V_{s,b}$ is the storage volume of freshwater [m^3] of water board b, t is time [s], E_b is the rate of freshwater extraction [m^{3}s^{-1}] of water board b as a function of t; and D_b the demand rate for freshwater [m^{3}s^{-1}] of water board b as a function of t.

For simplicity, the freshwater demand D_b is considered constant over time. Moreover, the supply of freshwater E_b is assumed to be fully accounted for by the water intake stations belonging to a water board. At each intake station i, the freshwater extraction rate fluctuates over time, as it is a function of the water and salinity levels. Water intakes can only extract water using gravity; that is, the water level in the river system must exceed a critical water level threshold, typically around the mean water level. Furthermore, water intakes can only extract water from the river system if salinity levels are below a certain limit; in the Netherlands, this limit is 150 mg Cl$^-$ l^{-1} (or 0.27 psu). Hence, freshwater extraction only occurs if these two criteria are met (Eqs. (2a) and (2b)):

$$\eta_i(t) > \eta_{\mathrm{threshold},i} \tag{2a}$$

$$s_i(t) < s_{\mathrm{limit},i} \tag{2b}$$

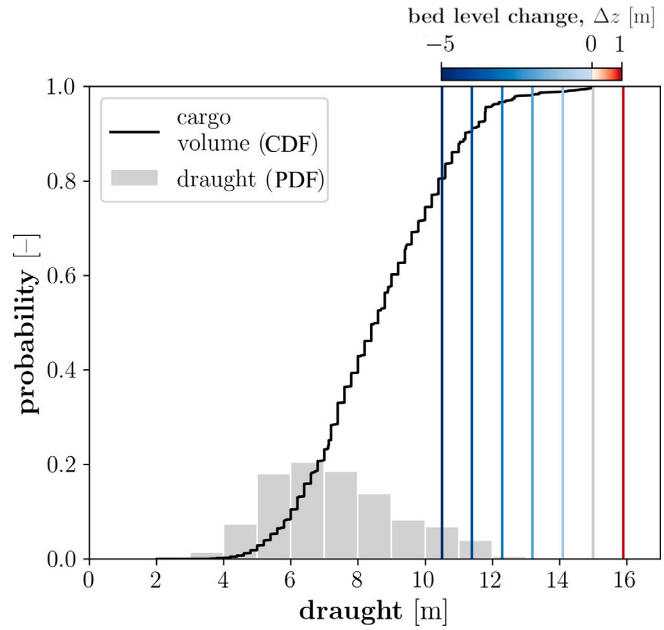

Fig. 5. Vessel draught and cargo volume distributions based on AIS data. Vertical, coloured lines represent the maximum allowable draught for each bed level change.

where η_i is the water level of the river [m] at water intake station i; $\eta_{\mathrm{threshold},i}$ the water level threshold [m] of water intake station i; s_i the salinity of the river [psu] at water intake station i; and $s_{\mathrm{limit},i}$ the salinity limit [psu] of water intake station i.

Expanding the supply term $E_b(t)$ into contributions from individual intake stations and including the constant freshwater demand $D_b(t)$ over time in Eq. (1) yields Eq. (3):

$$\frac{\mathrm{d}V_{s,b}}{\mathrm{d}t} = \sum_{i \in \mathcal{I}_b} E_i\Big(\eta_i(t), s_i(t)\Big) - \bar{D}_b \tag{3}$$

where E_i is the freshwater extraction rate [m^{3}s^{-1}] at intake station i, which depends on the water level $\eta_i(t)$ [m] at intake station i and salinity $s_i(t)$ [psu] at intake station i; $\mathcal{I}_b$ is the set of intake stations belonging to water board b; and $\bar{D}_b$ the time-averaged demand for freshwater [m^{3}s^{-1}] of water board b.

Based on a review of actual discharge curves of water intake stations, the model assumes that the extraction rate of freshwater E_i follows a binary relation (Eq. (4)) depending on Eqs. (2a) and (2b):

$$E_i\Big(\eta_i(t), s_i(t)\Big) = \begin{cases} E_{\max,i} & \text{if Eqs. (2a) \& (2b)} \\ 0 & \text{else} \end{cases} \tag{4}$$

where $E_{\max,i}$ is the maximum extraction rate [m^{3}s^{-1}] of water intake station i; E_i, $\eta_i(t)$, and $s_i(t)$ as previously defined.

A water board's storage volume, $V_{s,b}$ [m^3], is bounded by a minimum volume of zero and a maximum storage capacity, $V_{s,\max,b}$ (Eq. (5)):

$$0 \le V_{s,b} \le V_{s,\max,b} \tag{5}$$

where the variables are as defined previously.

Hence, the model requires the following input: the maximum storage capacity $V_{s,\max,b}$ [m^3] and the yearly average freshwater demand rate $\bar{D}_b$ [m^{3}s^{-1}] of each water board b, and the maximum extraction rate $E_{\max,i}$ [m^{3}s^{-1}], water level threshold $\eta_{\mathrm{threshold},i}$ [m], and salinity limit $s_{\mathrm{limit},i}$ [psu] of each water intake station i. The water level threshold and salinity limit are set to 0.0 m (relative to the local reference system: NAP) and 0.27 psu, respectively, for all water intake stations.

Table 1
Specifications of the main water intakes in the Rhine-Meuse Delta without emergency water supply—derived from van der Wijk (2020)—per water board. The labelling of the water boards and numbering of the water intakes reflect the locations numbered in Fig. 2. Numbers post-fixed with an asterisk are collectively considered at Krimpen aan de IJssel, marked in Fig. 2. $V_{s,max,b}$ is the water boards' maximum storage capacity, $\bar{D}_b$ is the water boards' time-averaged freshwater demand rate; and $E_{max,i}$ is the water intake stations' maximum extraction rate.

Water board		Intake station		$V_{s,max,b}$ [m^3]	$\bar{D}_b$ [m^{3}s^{-1}]	$E_{max,i}$ [m^{3}s^{-1}]
A.	Hollandse Delta	1	Inlaatsluis Spijkenisse	4,000,000	9.1	23.0
		2	Inlaatsluis Bernisse			23.0
B.	Delfland	(2)	Gemaal Winsemius	492,000	2.75	4.0
		3	Schiegemaal			3.0
C.	Schieland & Krimpenerwaard	4	Mr. U.G. Schilthuis	528,000	2.5	4.5
		5*	Snelle Sluis & Gemaal Abraham Kroes			3.3
		6*	Gemaal Verdoold	3,408,000	5.6	1.5
		†	Krimpenerwaard			5.6
D.	Rijnland	7*	Gouda	2,086,400	12.0	21.0

Water shortages occur when the demand exceeds the supply—or extraction rate—and the storage is empty. We define water shortage as the demand that cannot be provided by the combination of water supply and remaining available storage (Eq. (6)):

$$S_b(t) = \max\left[\bar{D}_b - E_b(t) - \max\left\{-\frac{\mathrm{d}V_{s,b}(t)}{\mathrm{d}t}, 0\right\},\ 0\right] \tag{6}$$

where S_b is the freshwater shortage rate [m^{3}s^{-1}] at water board b; t, $\bar{D}_b$, E_b, and $V_{s,b}$ as previously defined.

To apply the above metric to the situation in the RMD, we selected the main water intakes and their collections without emergency water supply based on van der Wijk (2020), which are presented in Table 1. Since the hydrodynamic model was found to poorly predict salinity in the Hollandsche IJssel, the main water intakes in this branch—marked with asterisks in Table 1—were evaluated based on the modelled hydrodynamic data at Krimpen aan de IJssel (Fig. 2). Furthermore, Gemaal Winsemius and Inlaat Bernisse used the same hydrodynamic data; and Krimpenerwaard was projected on hydrodynamic data at the mouth of the Lek—i.e. at Kinderdijk (marked with † in Fig. 2).

3.4. Performance indicators

Using the processing methods as described in Sections 3.2 and 3.3, we have defined performance indicators reflecting port functioning and freshwater availability. The indicators follow actual Key Performance Indicators (KPIs) for the stakeholders.

For the port, we used the common KPI of waiting rate (Eq. (7))—i.e. vessel trip delays over vessel trip time—expressing the level of maritime service and port competitiveness (Park et al., 2020):

$$\mathcal{P}_{port} = 1 - \frac{\sum_{k=1}^{N} V_{v,k} \cdot t_{w,k}}{\sum_{k=1}^{N} V_{v,k} \cdot t_{tr,k}} \tag{7}$$

where $\mathcal{P}_{port}$ is the performance indicator for port performance [–]; N is the number of vessels entering the port during the period of interest [–]; $V_{v,k}$ the vessel volume (cargo volume) [m^3] of vessel k; $t_{w,k}$ the waiting time [s] of vessel k; and $t_{tr,k}$ the trip time [s] of vessel k.

Herein, the trip time of a vessel is defined as the total time a vessel takes to unload its cargo after arriving at the port (or departing from a previous terminal) and to load new cargo and depart from the port (or arrive at a next terminal). This includes additional waiting time. The performance indicator, therefore, "permits" more waiting time for vessels with longer trip times and less cargo, thereby adjusting for (cost) efficiency. Within the port, however, vessel trip times across vessels are generally in the same order of magnitude.

A perfect port performance ($\mathcal{P}_{port} = 1$) would be achieved if no vessel has delays, i.e. vessel waiting times are zero. An affected port will experience cargo transshipment delays: a higher degree of delay on the total trip time results in a poorer operating (less competitive) port. Note that $\mathcal{P}_{port}$ is bounded by zero and, thus, cannot become negative: $\mathcal{P}_{port} \in (0, 1]$. We believe that this rational form can be comprehensive for decision-makers and the general public, as it can be interpreted as the degree of stakeholder satisfaction. Note that the performance indicator can also be calculated for each berth or terminal specifically.

The performance indicator related to the freshwater availability, $\mathcal{P}_{freshwater}$, reflects freshwater shortage and thereby the reliability of the supply system, a common KPI in freshwater supply (Carvalho de Matos Teixeira Coelho, 1996). A perfect performance ($\mathcal{P}_{freshwater} = 1$) is achieved when the water board can fulfil the freshwater demand at any time. Therefore, this performance indicator is a function of the freshwater shortage versus the demand, integrated over the period of interest (Eq. (8)):

$$\mathcal{P}_{freshwater} = 1 - \frac{\int_T S\ \mathrm{d}t}{\int_T D\ \mathrm{d}t} \tag{8}$$

where T is the period of interest [s]; S the freshwater shortage (Eq. (6)) [m^{3}s^{-1}]; and D the freshwater demand [m^{3}s^{-1}]. Note that $\mathcal{P}_{freshwater}$ is also bounded by zero, due to which it cannot become negative: $\mathcal{P}_{freshwater} \in [0, 1]$. Again, this rational form can be intuitive for decision-makers and the general public. Moreover, Eq. (8) can be applied to each water board b independently or collectively across multiple water boards using their sum of freshwater demand and supply.

The two defined performance indicators can be traded off using the method in Fig. 3. To maintain method comprehension and prevent running into politics, we use equal weighting of the objectives and do not apply prior valuation across the ranges of the performance indicators; we do not have prior insights into the weighting and valuation by the decision-maker and stakeholders. Nevertheless, weighting and valuation typically arise in trade-offs and can be incorporated into the method (see Eq. (9) in Section 5.3).

We assessed the trade-off using multi-objective optimisation, which leads to the generation of Pareto-optimal solutions (e.g., Emmerich and Deutz, 2018). This set of solutions consists of the performance indicators for each stakeholder per bed level change scenario. Assuming linear behaviour between these outcomes, a trade-off curve can be constructed through interpolation. The trade-off curve cannot be further improved upon (e.g., Deb, 2001); a so-called *a posteriori* method to inform decision-makers about the optimal alternatives without making a choice *a priori* (Miettinen, 1998). Note that this approach results in a collection of optimal solutions, not a single "optimal solution". Here, "optimal" refers to the best trade-off between the chosen performance indicators, which is at best as good as the indicators themselves. For simplicity, this study focuses on a single trade-off curve between the interests of the bed level change affected terminals of the PoR jointly and the collective water boards. However, trade-off curves of individual water boards are also quantified.

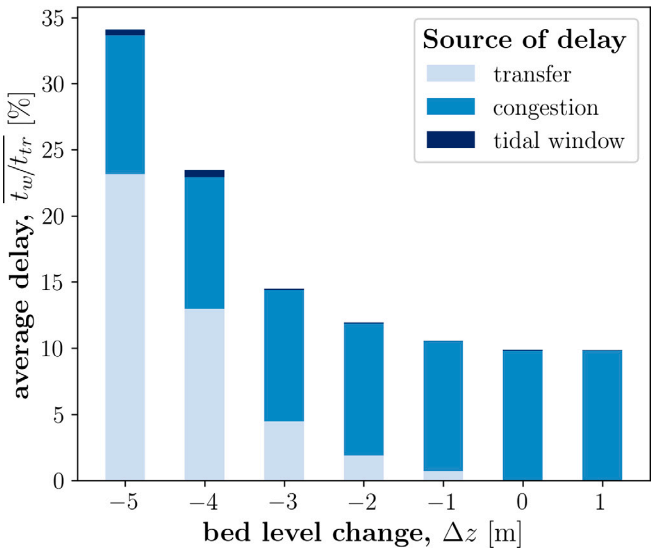

Fig. 6. Contribution of the delay time to the total cargo transfer time caused by transferring cargo between vessels, berth congestion, and tidal windows.

4. Results

4.1. Delayed throughput

The AIS data analysis revealed that 90.8% of the vessel trips calling at the selected terminals are not affected by a shallower NWW of 11.5 m ($\Delta z = -5$ m, Fig. 5). Notably, vessels with draughts greater than 12.0 m undertake less than 1.0% of the total trips, and are therefore not clearly visible in the draught distribution of Fig. 5. However, since larger, deeper-draughted vessels transport relatively more cargo, we observe that up to 22.9% of the cargo has to be transferred to the replacement coasters (for $\Delta z = -5$ m). The shallower the NWW, the greater the number of deep-draughted vessels that are impeded from navigating this channel, the more trips are required with replacement coasters.

In line with this observation, the nautical traffic model predicts that the inland part of the PoR is highly affected by a shallower NWW (Fig. 6): the average delivery time increases with a shallower NWW. This is mainly caused by the additional delay of transferring cargo to the replacement coasters, which increases with shallower MBLs. Consequently, the waiting rate increases, decreasing the port's performance. In addition, extra congestion arises as more vessels are required to transship the same amount of cargo—i.e. the additional replacement coasters. Delays due to tidal restrictions are also increasing, as with shallower depths more vessels rely on tidal windows. However, this is only a marginal effect.

In contrast, we observed that a deeper NWW will not lead to a substantially better performing port for the current fleet of call. Although the delays due to tidal restrictions slightly decrease, the port remains subject to congestion of berths. In other words, given the current bed levels, congestion is the dominating factor of delay in the port.

4.2. Water shortages

The results of the freshwater supply model are presented in Fig. 7. The model predicts that the overall freshwater availability improves with shallower bed levels; freshwater shortages decrease. Note that the shortages in Fig. 7 are expressed in volume per area, which causes the summation of shortages of all four water boards to be less than the sum of all water boards. In essence, these numbers resemble rainfall deficits, which range between virtually zero (Fig. 7c and d) to shy of 0.2 m (Fig. 7e) with the current MBL (16.2 m). Generally, the water boards become more robust to a drop in the discharge of the NWW with shallower bed levels. This improves the starting position at the beginning of the drought and postpones and reduces the effects of the drought on the water intakes.

For the water boards in specific, the Delfland and Hollandse Delta water boards are the least susceptible to the drought conditions in their freshwater availability (Fig. 7b and c) despite being closest to the sea (Fig. 2). The influence of reducing the MBL is, therefore, also least profound in these water boards. The other two water boards, however, show a greater dependence between freshwater shortages and the MBL (Fig. 7d and e). This is related to the source of freshwater extraction: the Delfland and Hollandse Delta water boards mainly extract from the man-made freshwater lake in the southern RMD—the Haringvliet and the connected Brielse Meer—which is more robust to droughts (Fig. 1). The other two water boards are more reliant on freshwater from the northern RMD, which is more strongly affected by droughts and changes in the water depth of the NWW.

In contrast to the above, further deepening the NWW (i.e. $\Delta z = +1.0$ m) barely affects the freshwater availability with respect to the reference case (i.e. $\Delta z = \pm 0.0$ m). It is only at the Schieland & Krimpenerwaard water board where deepening results in a minor increase in freshwater shortage (Fig. 7e).

4.3. Pareto front

Fig. 8 presents the obtained trade-off curves between the performances of the port, $\mathcal{P}_{\text{port}}$, and the water boards, $\mathcal{P}_{\text{freshwater}}$. The shape of the trade-off curves aligns with the modelling results. The port performance drops significantly with shallower bed levels, particularly from $\Delta z = -3.0$ m onwards. On the other hand, the joint performance of the water boards improves step-wise with decreasing MBL. The port performance seems more impacted by shallower MBLs than the collective performance of the water boards, shown by the angle of the Pareto front and the range of the values covered. However, the trade-off curve differs per water board. The performance of the Delfland and Hollandse Delta water boards is barely impacted by the MBL, which aligns with their largely unaffected freshwater shortages (Fig. 7c and d). In contrast, the performance of the Schieland & Krimpenerwaard and Rijnland water boards is more or less equally heavily impacted as the performance of the port, aligning with their severely impacted freshwater shortage (Fig. 7e and f).

Furthermore, the increase in port performance with a deeper NWW beyond the MBL of 16.2 m is limited, given the current fleet composition (Fig. 8). This is in line with the expectations from the results of the nautical traffic model. Although the accessibility of the port increases—delays due to tidal windows decrease (Fig. 6)—few vessels benefit from deeper MBLs (Fig. 5). In addition, a deeper NWW results in a negligible impact on the performance of the water boards. This corresponds with the results from the freshwater supply model, predicting comparable freshwater shortages for the reference and deepening scenarios (Fig. 7).

5. Discussion

The MBL in the NWW has a profound influence on the performance indicators of both the port and the water boards, resulting in a Pareto front (Fig. 8). The resulting trade-off curve is illustrative but also sensitive to assumptions. Therefore, this section reflects on the underlying assumptions in the framework setup and application, including the design of the performance indicators and model simplifications (Section 5.1). Hereby, we focus on the concepts of completeness, transparency, and advocacy, as described by Keeney and Raiffa (1993). In addition, this section further emphasises the significance of the results for implementing effective draught countermeasures beyond shallowing (Section 5.2), and the broader potential of the framework in policy and decision-making through Pareto valuation (Section 5.3).

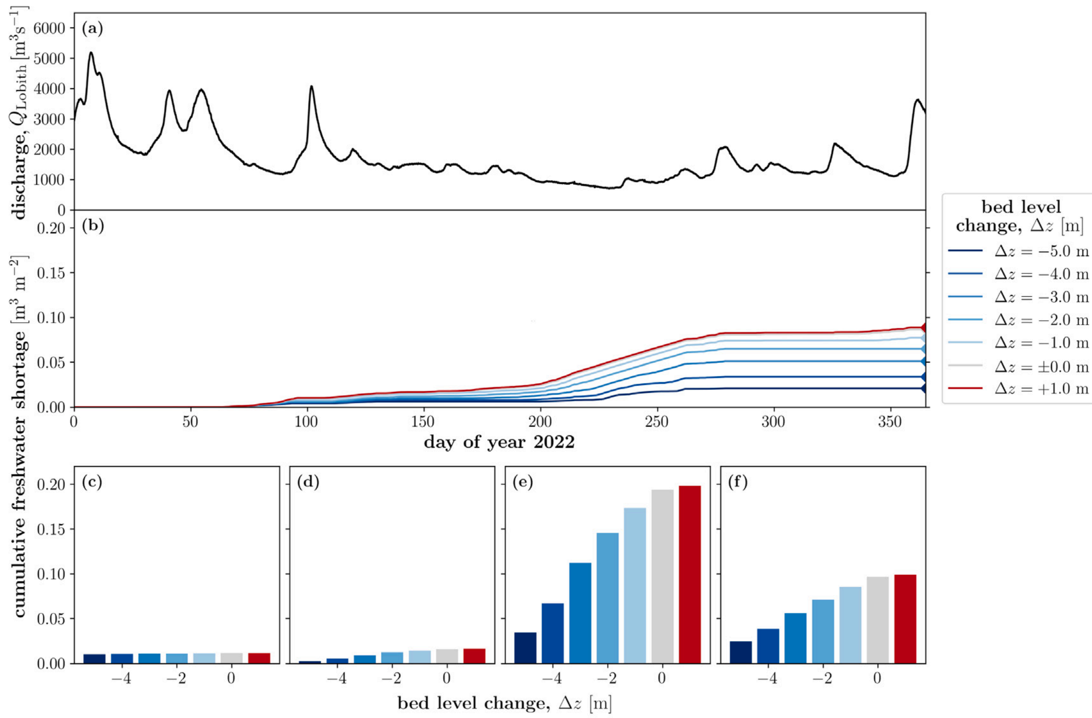

Fig. 7. The influence of the MBL on the water shortages. **(a)** Discharge at Lobith; **(b)** temporal development of cumulative water shortages for all water boards; and cumulative water shortages per water board: **(c)** Delfland, **(d)** Hollandse Delta, **(e)** Schieland & Krimpenerwaard, and **(f)** Rijnland. Shortages are expressed as defined by Eq. (6).

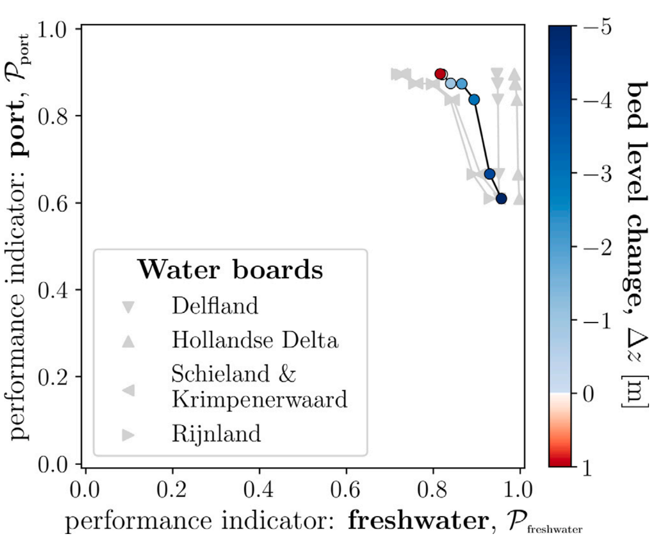

Fig. 8. Pareto front of the stakeholder performance indicators as a function of the water depth. The collective is shown as the black line with dots coloured by bed level change, and individual water boards are presented in grey.

5.1. Trade-off curve uncertainty and sensitivity

The choice of the framework's underlying models and definition of the performance indicators influences the shape of the Pareto front. Models are always "wrong" in the sense that they are simplifications of reality, and thereby inherently incomplete. Moreover, model assumptions and definitions of performance indicators generally include some form of advocacy—although not always intentionally. In this subsection, we reflect on the most impactful modelling decisions within the overall framework.

First, this study has implemented a relatively simple hydrodynamic model designed to assess water levels and current velocities accurately. Although the model yields relatively fast results with satisfactory predictions regarding salinity for the reference situation (Fig. 4), there remains some uncertainty whether the underlying processes for salt intrusion are sufficiently represented to rely on the outcomes of the scenario runs (Kranenburg et al., 2015). The model's underestimation of the saltwater intrusion could have resulted in a more profound impact on the performance of the water boards. In addition, the model's poor predictive power regarding salinity inside smaller branches of the RMD—where local freshwater discharges and extractions become dominant—and the subsequent assumptions could have impacted the results. Therefore, to improve the accuracy of the results, we advise using a more detailed hydrodynamic model for direct implementation and cross-validation of the simpler *OSR* model (Fig. 2; e.g., Geraeds et al., 2025; Gerritsma, Avelon Verlaan et al., 2025, describe detailed hydrodynamic models focused on salt dynamics in the RMD). Note, however, that the implementation of such models comes at higher computational costs, which might further complicate the application of the framework.

Second, the predicted waiting times are highly dependent on the setup of the nautical traffic model and its underlying assumptions—particularly the maintained cargo throughput to the inland terminal by smaller replacement vessels and the choice of replacement vessel type. The model neglects tugs, pilots, background traffic, and terminal cargo flows, which affects the nautical traffic behaviour (Bakker et al., 2024b), and could have resulted in a more impacted port performance. Furthermore, the nautical traffic model and the port performance indicator (Eq. (7)) were highly dependent on AIS data as input. Although generally of good quality, GPS location errors could have resulted in modelling discrepancies in terms of erroneous vessel laytimes and speeds. Moreover, as vessel dimensions in the AIS data are known to be susceptible to uncertainty—especially the exact hull shape and draught, which is sometimes purposefully underreported (Meyers et al., 2022) and affected by intake of ballast water—the calculation of the cargo volumes and number of required replacement vessels includes errors, directly affecting the port performance indicator. Therefore, further improvements to the nautical traffic model and AIS data analysis are recommended, preferably by engaging with stakeholders and experts. The open-source OpenTNSim simulation library enables these improvements. Despite the above assumptions and possible errors, we believe that the state-of-the-art nautical model performed as intended, and the resulting levels of port performance are trustworthy.

Third, the use of a simple freshwater volume-balance model may have affected the estimation of the performance indicator for freshwater availability—i.e. Eq. (8). The model strongly depends on the quality of the hydrodynamic model's salinity predictions. Furthermore, the model simplifications—i.e. the time-constant freshwater demand, single water level thresholds and salinity limits, and the exclusion of precipitation—could have led to discrepancies with reality. The model is sensitive to its input parameters—particularly the extraction rates of the water intake stations and the freshwater demand of the water boards. Despite these simplifications, the results are in accordance with experienced shortages reported by van der Wiel et al. (2021). However, further model improvements based on engagement with stakeholders and experts are recommended to improve the completeness of the decision problem in future research.

Fourth, the defined performance indicators—although according to our best understanding of the problem and purposefully designed as objective, non-monetary metrics to describe the interests of the stakeholders as closely as possible—inevitably have been subject to some advocacy. Other performance indicators could have been used, e.g., processed cargo throughput or cumulative freshwater shortage. In addition, the scope of focusing on the bi-objective decision problem between the interests of ports and water boards limits the decision objective space for this particular application. The above choices could easily have influenced the interpretation of the trade-off curve. However, the presented trade-off method is transparent—if underlying modelling results are reported adequately—and flexible to support other sets of performance indicators and can also include more stakeholders. Hereby, the objective is to achieve a unanimous and complete understanding and interpretation of the decision space, reducing advocacy and bias. Such an approach requires engagement of the stakeholders, experts, and decision-makers to achieve a unanimous and complete interpretation of the trade-off. Note, however, that the performance indicators implemented remain metrics and, thereby, inherently incomplete (Muller, 2021).

At last, we only assessed the trade-off for the year 2022, which contained a severe drought resulting in an "extremely rare low flow" in the Rhine (Toreti et al., 2022; Wegman et al., 2025), while the shape of the trade-off curve is sensitive to the environmental and socioeconomic conditions—e.g., a dry versus a wet year, or a quiet versus a busy year in terms of nautical traffic. As decisions must be made for a defined horizon—i.e. the lifetime of an intervention—future application of the framework should account for such sensitivity in hydrodynamic forcing and socioeconomic developments. For example, bed level designs are typically made for the coming tens of years, as capital and maintenance dredging costs and underlying contracts are involved, thereby impacting stakeholders for this complete horizon. Therefore, future-proof decision-making cannot rely on a hindcast assessment of a single year—e.g., 2022. Instead, the trade-off curve should be probabilistic—i.e. an expected trade-off curve with an associated bandwidth based on which a final curve can be established using risk analysis—incorporating uncertainty over the entire decision horizon, including that arising from climate change (e.g., sea level rise and more severe, prolonged droughts) and socioeconomic trends (e.g., increased freshwater demand and the use of more and/or deeper-draughted vessels). On the one hand, this necessitates a sensitivity analysis on model parameters and underlying assumptions and definitions of performance indicators. On the other hand, this requires various realistic external boundary conditions for the underlying models—e.g., time series of (extreme) discharges, various degrees of sea level rise, various fleet compositions, and changing water demand. A downside of this approach is the involved computational cost of having many simulation runs, as uncertainty propagates from the hydrodynamic model to the stakeholder impact assessment models. Therefore, fast models should be typically used for this, combined with a limited simulation period—e.g., the duration of a drought, or the month of normative nautical traffic. Moreover, adaptive sampling machine learning techniques (e.g, Hendrickx et al. (2023b)) that dynamically explore the decision space could assist in downscaling the problem dimensions, focusing on the most profound uncertainties and most sensitive parameters.

5.2. Drought countermeasures

Despite the possible crude model assumptions and omission of sensitivity and uncertainty, the modelling results and trade-off curve provide useful and transparent information for optimising the joint performance of stakeholders in the RMD. For example, the relative marginal impact on port performance for a 1.0 m shallower NWW ($\Delta z = -1.0$ m) could be beneficial for the port in reducing the dredging requirements. Moreover, while shallower bed levels seem to significantly improve the resilience of freshwater supply, a MBL of 11.2 m would not even be sufficient to protect all water boards in the RMD from water shortages during a severe drought such as in 2022 ($\Delta z = -5.0$ m in Fig. 7). Thus, additional measures to secure drinking water safety are required; the alternative water supply system in place in the Netherlands to cope with extreme drought conditions by relocating freshwater between water boards—a plan that was also successfully employed during the drought in 2022 (van der Heijden et al., 2024)—remains critical for the years to come, although this might not be a robust solution in the long term. This claim was validated with our freshwater supply model, as including the alternative water supply system would lead to no freshwater shortages.

In addition to—or instead of—such a system, more robust and permanent measures could be taken to enhance the resilience of the freshwater supply to climate change and socioeconomic developments. Regarding the freshwater availability, there are four components that can alleviate the stress during droughts: (1) increase the freshwater storage capacity (V_c); (2) increase the maximum extraction rate ($E_{\max}$); (3) reduce the freshwater demand (D); and/or (4) move water intakes away from salt-sensitive regions. Note that these components should not be considered in isolation, but can be combined to establish a resilient freshwater management system. The last component is also what makes the Delfland and Hollandse Delta water boards relatively insensitive to the MBL of the NWW: these water boards extract the majority of their freshwater from the southern RMD—namely the man-made, freshwater lake Haringvliet. Current plans to reconnect the Haringvliet with the North Sea by (partially) opening the Haringvliet sluices (Brevé et al., 2019; Reeze et al., 2022) can lead to increased salinisation (Kranenburg et al., 2023) and should therefore be carefully assessed (Hendrickx et al., in prep). In addition, other (nature-based) measures can be taken to reduce saltwater intrusion—i.e. Chen et al. (2025)—that may be less impactful for port performance.

5.3. Performance valuation

The Pareto front in Fig. 8 transparently and intuitively shows the trade-off between the port and freshwater performances arising from modifying the MBL and is useful in policy and decision-making. Given the front, the mathematically optimal solution can, amongst other methods, be achieved by maximising the square area below the Pareto front, the sum of the performance indicators, the point of maximum steepness of the Pareto front, or the minimal distance of the curve to a selected point optimum (e.g., Emmerich and Deutz, 2018). For example, in this study, an optimum of a bed level change of −2.0m is found for the collective trade-off curve. The optimum for individual

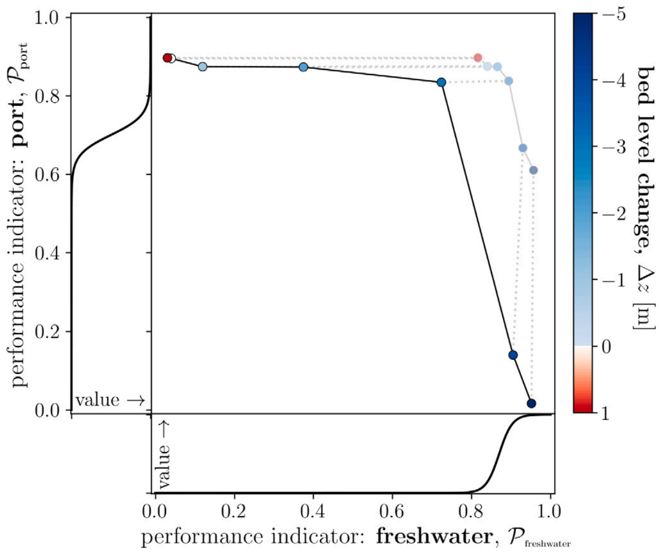

Fig. 9. Valued Pareto front based on arbitrary valuation functions using Eq. (9). The unvalued Pareto front is faded and presents the same data as in Fig. 8.

water boards, however—e.g., Schieland & Krimpenerwaard and Rijnland, which are more impacted by the bed level of the NWW—the optimum shifts towards −3.0m. Note that these numbers are first estimates, given the possible crude model assumptions, lack of uncertainty quantification, and incomplete decision space, and should, therefore, not be adopted yet.

To actually "use" the trade-off curve in policy and decision-making, it should include the valuation of the solution space by stakeholders and the bias of the decision-maker in terms of weighting factors of the performance indicators in terms of preference based on stakeholder influence or importance. Such weighting and valuation are subjective and part of the policy and decision-making process. In general, the valuation of each individual performance indicator is nonlinear, and can put limits on the allowable performance values. To maintain the intuitive visualisation of the Pareto front, the weighting and valuation can be included by means of weighting factors and valuation functions, respectively (Eq. (9)):

$$\mathcal{V}_p(\vec{x}) = w_p \cdot v_p(\mathcal{P}_p) \cdot \mathcal{P}_p(\vec{x}) \tag{9}$$

where $\mathcal{V}_p$ is the valued performance indicator p [–]; w_p is a weighting factor of the decision-maker for each performance indicator p [–]; v_p the valuation function of performance indicator p [–]; $\mathcal{P}_p$ the (unvalued) performance indicator p [–]; and $\vec{x}$ the design parameter(s).

A transformation of the collective Pareto front (Fig. 8), using valuation functions, is presented in Fig. 9. Note that these valuation functions are arbitrarily defined and intended as examples of how they transform the Pareto front. A minimum performance can be enforced by setting a very low valuation for performances below this minimum; e.g., in Fig. 9, the port performance and freshwater supply performance are required to be $\mathcal{P}_{port} \geq 0.6$ and $\mathcal{P}_{freshwater} \geq 0.8$ respectively (approximately).

Although the valuation functions in Fig. 9 are both smooth, tipping points that are relevant for stakeholders may arise and can be reflected by discontinuities in the functions. As the definition of such a valuation function is subjective, political, and subject to the zeitgeist, we have only included example valuation functions in Fig. 9 and refer to Keeney and Raiffa (1993) and Greco et al. (2016) for methods to define such functions, which are intended to reflect the stakeholder interests through stakeholder engagement.

Figs. 8 and 9 illustrate how insightful and intuitive the use of Pareto fronts is in policy and decision-making; they clearly show the trade-offs associated with the policies and decisions at stake. These features make such visualisations also useful in communicating the policy and decision-making process with the public, who are generally not experts in the field but are highly affected by the policies and decisions being made. This is particularly useful in digital twins (Wannasin et al., 2024), integrated assessment models (Pourteimouri et al., 2024), and serious games (den Haan et al., 2020, 2024).

Although we have limited ourselves to two performance indicators and one design parameter in this study, the presented approach—i.e. the use of design parameters, performance indicators and a Pareto front—can easily be upscaled to multiple dimensions (e.g., Emmerich and Deutz, 2018). Note that with increasing dimensionality, visualising the trade-offs might become harder due to the human visual limit of three dimensions. Moreover, the construction of a complex multidimensional Pareto front requires lots of Pareto points, and hence lots of model simulations. Therefore, an effective sampling method—e.g., an adaptive sampling approach—could be used to limit the number of (expensive) model simulations (Gramacy and Lee, 2009; Hendrickx et al., 2023a). Additionally, computationally efficient hydrodynamic and stakeholder models can be employed, which may come at the cost of precision and resolution. For example in this research, the idealised and simplified saltwater intrusion model of Biemond et al. (2024) could become useful in a fast prediction of the freshwater availability performance; the nautical traffic and freshwater supply models applied in this paper are deemed sufficiently computationally efficient.

At last, we would like to highlight the general applicability and usefulness of the trade-off method approach in other case studies. An example is the decision on partially opening of the Haringvliet sluices in which freshwater availability and ecology have to be traded off (Section 5.2; Hendrickx et al., in prep). Other examples may contain the future design and management of the highly urbanised and strongly stressed RMD and other worldwide deltas. Especially here, we foresee that the presented system-scale and objective approach would be a highly effective tool for policy and decision-makers in obtaining the most effective solutions given the most urgent of challenges.

6. Conclusion

In this study, we assembled a general framework to explore the socioeconomic implications of bed level change of the Rhine-Meuse Delta's primary outlet channel, considering the severely dry year of 2022. Thereby, we assessed the trade-off of the dissimilar, conflicting interests of the two major stakeholders in the area: (1) the Port of Rotterdam, located at the mouth of the delta, that uses the channel as its main deep waterway route; and (2) the water authorities extracting freshwater from the inland delta, i.e. the water boards. The framework requires carefully selected objective, non-monetary performance indicators to quantify the trade-off using Pareto optimisation. These indicators were calculated based on two separate stakeholder impact assessment models, namely a nautical traffic model and freshwater supply model. The models were fed with the output of a hydrodynamic model and other operational data, such as vessel tracking data and properties of the main freshwater intake stations. Thus, a link was created between the physical system and the performance of the stakeholders; by varying the bed level of the channel in the hydrodynamic model, we obtained the impact on the stakeholder performance indicators. This resulted in a Pareto front showing that shallower bed levels deteriorate port accessibility, while improving freshwater availability (Fig. 8).

We have shown that the obtained Pareto fronts provide valuable insights into the trade-offs of interventions in any multidisciplinary setting. Although this study has limited its multidisciplinary assessment to two stakeholders, this approach can easily be extended to multiple dimensions—i.e. multiple stakeholders with multiple objectives. The

Pareto front is a visually intuitive way of showcasing the benefits and costs of various scenarios for different stakeholders. With the use of valuation functions, the Pareto front can be transformed to represent performance values, maintaining the intuitive visual representation of Pareto fronts (Fig. 9). These characteristics make Pareto fronts useful tools for policy and decision-makers, as well as for communicating with the public.

CRediT authorship contribution statement

Floor P. Bakker: Writing – original draft, Visualization, Validation, Software, Methodology, Investigation, Formal analysis, Data curation, Conceptualization. **Gijs G. Hendrickx:** Writing – original draft, Visualization, Validation, Methodology, Investigation, Formal analysis, Data curation, Conceptualization. **Lennart M. Keyzer:** Writing – review & editing, Resources. **Sebastian R. Iglesias:** Writing – review & editing, Methodology, Conceptualization. **Stefan G.J. Aarninkhof:** Writing – review & editing, Supervision, Project administration, Funding acquisition, Conceptualization. **Mark van Koningsveld:** Writing – review & editing, Supervision, Project administration, Funding acquisition, Conceptualization.

Acknowledgements

We would like to thank Lamber Hulsen (Port of Rotterdam) for his contributions to the early stages of this research.

Software availability

Port logistics were modelled using OpenTNSim (Bakker et al., 2024a).

Funding

This publication is part of the project "Design and operation of nature-based SALTISolutions" (with project number P18-32 Project 7) of the research programme SALTISolutions which is (partly) financed by the Dutch Research Council (NWO).

Declaration of competing interest

The authors declare the following financial interests/personal relationships which may be considered as potential competing interests: Floor P. Bakker reports financial support was provided by Dutch Research Council. Gijs G. Hendrickx reports financial support was provided by Dutch Research Council. Lennart Keyzer reports a relationship with Port of Rotterdam Authority that includes: employment. Sebastian Iglesias reports a relationship with Royal Van Oord BV that includes: employment. Mark van Koningsveld reports a relationship with Royal Van Oord BV that includes: employment. Stefan Aarninkhof reports a relationship with PUB Singapore's National Water Agency that includes: consulting or advisory. Stefan Aarninkhof reports a relationship with Stichting EcoShape Building with Nature that includes: board membership. Stefan Aarninkhof reports a relationship with Rijkswaterstaat, Expertise Netwerk Waterveiligheid that includes: board membership. Stefan Aarninkhof reports a relationship with Rijkswaterstaat, Dutch Coastline Challenge that includes: board membership. Stefan Aarninkhof reports a relationship with Stichting Waterbouw that includes: board membership. If there are other authors, they declare that they have no known competing financial interests or personal relationships that could have appeared to influence the work reported in this paper.

Data availability

Data will be made available on request.

References

Alcamo, J., Flörke, M., Märker, M., 2007. Future long-term changes in global water resources driven by socio-economic and climatic changes. Hydrol. Sci. J. 52 (2), 247–275. http://dx.doi.org/10.1623/hysj.52.2.247.

Almaz, O.A., Altiok, T., 2012. Simulation modeling of the vessel traffic in delaware river: Impact of deepening on port performance. Simul. Model. Pr. Theory 22, 146–165. http://dx.doi.org/10.1016/j.simpat.2011.12.004.

Baart, F., Jiang, M., Bakker, F.P., Frijlink, T., van Koningsveld, M., 2022. OpenTNSim v1.2.0. http://dx.doi.org/10.5281/zenodo.7053274, Zenodo.

Bakker, F.P., Baart, F., van Koningsveld, M., 2024a. OpenTNSim v1.4.0-paper.3. http://dx.doi.org/10.5281/zenodo.11489436, Zenodo.

Bakker, F.P., van Koningsveld, M., 2023. Optimizing bed levels in ports based on port accessibility. In: Cox, D. (Ed.), Coastal Engineering Proceedings. (37), Sydney, Australia, http://dx.doi.org/10.9753/icce.v37.papers.62.

Bakker, F.P., van der Werff, S., Baart, F., Kirichek, A., de Jong, S., van Koningsveld, M., 2024b. Port accessibility depends on cascading interactions between fleets, policies, infrastructure, and hydrodynamics. J. Mar. Sci. Eng. 12 (6), 1006. http://dx.doi.org/10.3390/jmse12061006.

Beersma, J.J., Buishand, T.A., Buiteveld, H., 2004. Droog, Droger, Droogst. Technical Report, KNMI/RIZA, URL: https://cdn.knmi.nl/system/data_center_publications/files/000/044/486/original/publ_199ii_fase2_copy1.pdf?1432895246.

Best, J., 2019. Anthropogenic stresses on the world's big rivers. Nat. Geosci. 12 (1), 7–21. http://dx.doi.org/10.1038/s41561-018-0262-x.

Biemond, B., Kranenburg, W., Huismans, Y., de Swart, H.E., Dijkstra, H.A., 2024. Dynamics of salt intrusion in complex estuarine networks: An idealised model applied to the rhine-Meuse Delta. http://dx.doi.org/10.5194/egusphere-2024-2322, EGUsphere, preprint.

Breine, J., Maes, J., Ollevier, F., Stevens, M., 2011. Fish assemblages across a salinity gradient in the Zeeschelde estuary (Belgium). Belgian J. Zool. 141 (2), 21–44, URL: https://belgianjournalofzoology.eu/index.php/BJZ/article/view/148/229.

Brevé, N.W.P., Vis, H., Breukelaar, A.W., 2019. Escape from the North Sea: the possibilities for pikeperch (Sander lucioperca L. 1758) to re-enter the Rhine and Meuse estuary via the Haringvlietdam, as revealed by telemetry. J. Coast. Conserv. 23 (1), 239–252. http://dx.doi.org/10.1007/s11852-018-0654-5.

Buitink, J., Tsiokanos, A., Geertsema, T., ten Velden, C., Bouaziz, L., Spema Weiland, F., 2023. Implications of the KNMI'23 Climate Scenarios for the Discharge of the Rhine and Meuse. Technical Report, Deltares, Delft, the Netherlands, URL: https://www.deltares.nl/expertise/publicaties/implications-of-the-knmi23-climate-scenarios-for-the-discharge-of-the-rhine-and-meuse-2.

Carvalho de Matos Teixeira Coelho, S., 1996. Performance Assessment in Water Supply and Distribution (Ph.D. thesis). Heriot-Watt University, URL: https://www.ros.hw.ac.uk/handle/10399/1297.

Chen, W., Borsje, B.W., Roos, P.C., Hendrickx, G.G., Siemes, R.W.A., van der Sande, W., Bootsma, J., Saccon, E., Bakker, F.P., Hulscher, S.J.M.H., 2025. The effectiveness of nature-based solutions in mitigating salt intrusion in estuaries: A review. (in review).

Chen, Q., Zhu, J., Lyu, H., Pan, S., Chen, S., 2019. Impacts of topography change on saltwater intrusion over the past decade in the Changjiang Estuary. Estuar. Coast. Shelf Sci. 231, 106469. http://dx.doi.org/10.1016/j.ecss.2019.106469.

Cordier, M., Agúndez, J.A.P., O'Connor, M., Rochette, S., Hecq, W., 2011. Quantification of interdependencies between economic systems and ecosystem services: An input–output model applied to the seine estuary. Ecol. Econom. 70, 1660–16071. http://dx.doi.org/10.1016/j.ecolecon.2011.04.009.

Cox, J.R., Leuven, J.R.F.W., Pierik, H.J., van Egmond, M., Kleinhans, M.G., 2022. Sediment deficit and morphological change of the Rhine-Meuse river mouth attributed to multi-millennial anthropogenic impacts. Cont. Shelf Res. 244, 104766. http://dx.doi.org/10.1016/j.csr.2022.104766.

Dada, O.A., Li, G., Qiao, L., Ding, D., Ma, Y., Xu, J., 2016. Seasonal shoreline behaviours along the arcuate Niger Delta coast: Complex interaction between fluvial and marine processes. Cont. Shelf Res. 122, 51–67. http://dx.doi.org/10.1016/j.csr.2016.03.002.

de Nijs, M.A.J., Pietrzak, J.D., Winterwerp, J.C., 2011. Advection of the salt wedge and evolution of the internal flow structure in the Rotterdam Waterway. J. Phys. Oceanogr. 41 (1), 3–27. http://dx.doi.org/10.1175/2010JPO4228.1.

de Nijs, M.A.J., Winterwerp, J.C., Pietrzak, J.D., 2009. On harbour siltation in the fresh-salt water mixing region. Cont. Shelf Res. 29 (1), 175–193. http://dx.doi.org/10.1016/j.csr.2008.01.019.

de Vet, P.L.M., van Prooijen, B.C., Wang, Z.B., 2017. The differences in morphological development between the intertidal flats of the Eastern and Western Scheldt. Geomorphology 281, 31–42. http://dx.doi.org/10.1016/j.geomorph.2016.12.031.

de Vries, I., 2014. Toetsing Robuustheid Brielse Meer Voor Zoetwatervoorziening. Technical Report, Deltares, Delft, the Netherlands.

Deb, K., 2001. Multi-Objective Optimization using Evolutionary Algorithms. Wiley, URL: https://www.egr.msu.edu/~kdeb/papers/k2011003.pdf.

den Haan, R.J., Biemond, B., Baart, F., 2024. Using an idealized network model as the physical module for a salt intrusion serious game. In: Niesten, I., Tahsin, N., van Grootheest, D., Barneveld, H., Waldschläger, K., Hoitink, T. (Eds.), NCR Days 2024. Netherlands Centre for River Studies, Wageningen, the Netherlands, pp. 58–59, URL: https://pure.tudelft.nl/ws/portalfiles/portal/178129577/Using_an_idealized_network_model_as_the_physical_module_for_a_salt_intrusion_serious_game.pdf.

den Haan, R., van der Voort, M., Baart, F., Berends, K., van den Berg, M., Straatsma, M., Geenen, A., Hulscher, S., 2020. The Virtual River Game: Gaming using models to collaboratively explore river management complexity. Environ. Model. Softw. 134, 104855. http://dx.doi.org/10.1016/j.envsoft.2020.104855.

Distefano, T., Kelly, S., 2017. Are we in deep water? Water scarcity and its limits to economic growth. Ecol. Econom. 142, 130–147. http://dx.doi.org/10.1016/j.ecolecon.2017.06.019.

Emmerich, M.T.M., Deutz, A.H., 2018. A tutorial on multiobjective optimization: Fundamentals and evolutionary methods. Nat. Comput. 17 (3), 585–609. http://dx.doi.org/10.1007/s11047-018-9685-y.

Fagerburg, T.L., Alexander, M.P., 1994. Underwater Sill Construction for Mitigating Salt Wedge Migration on the Lower Mississipi River. Technical Report, Hydraulic Laboratory, US Army Engineer Waterways Experiment Station, Vicksburg, MS, USA, URL: https://apps.dtic.mil/sti/tr/pdf/ADA282894.pdf.

Figueroa, S.M., Lee, G., Chang, J., Jung, N.W., 2022. Impact of estuarine dams on the estuarine parameter space and sediment flux decomposition: Idealized numerical modeling study. J. Geophys. Res.: Ocean. 127, http://dx.doi.org/10.1029/2021JC017829.

Folke, C., Carpenter, S., Elmqvist, T., Gunderson, L., Holling, C.S., Walker, B., 2002. Resilience and sustainable development: Building adaptive capacity in a world of transformations. AMBIO: A J. Hum. Environ. 31 (5), 437–440. http://dx.doi.org/10.1579/0044-7447-31.5.437.

Garmendia, E., Gamboa, G., Franco, J., Garmendia, J.M., Liria, P., Olazabal, M., 2010. Social multi-criteria evaluation as a decision support tool for integrated coastal zone management. Ocean & Coastal Management 53, 385–403. http://dx.doi.org/10.1016/j.ocecoaman.2010.05.001.

Geraeds, M.E.G., Pietrzak, J.D., Gerritsma, A., Verlaan, M., Katsman, C.A., 2025. Assessing the importance of the near-field plume state on estuarine dynamics under varying wind conditions. J. Geophys. Res.: Ocean. http://dx.doi.org/10.22541/essoar.174534309.94419306/v1, (submitted for publication).

Gerritsma, Avelon Verlaan, M., Geraeds, M.E.G., Huismans, Y., Pietrzak, J.D., 2025. The effects of a storm surge event on salt intrusion: Insights from the rhine-Meuse Delta. J. Geophys. Res.: Ocean. http://dx.doi.org/10.1029/2024JC021520.

Gramacy, R.B., Lee, H.K.H., 2009. Adaptive design and analysis of supercomputer experiments. Technometrics 51 (2), 130–145. http://dx.doi.org/10.1198/TECH.2009.0015.

Greco, S., Figueira, J.R., Ehrgott, M. (Eds.), 2016. Multiple Criteria Decision Analysis: State of the Art Surveys, second ed. Springer, p. 1338, https://link.springer.com/book/10.1007/978-1-4939-3094-4.

Hansen, D.V., Rattray Jr., M., 1965. Gravitational circulation in straits and estuaries. J. Mar. Res. 23, 104–122, URL: https://elischolar.library.yale.edu/journal_of_marine_research/1048/.

Hendrickx, G.G., Antolínez, J.A.A., Herman, P.M.J., 2023a. Predicting the response of complex systems for coastal management. Coast. Eng. 182, 104289. http://dx.doi.org/10.1016/j.coastaleng.2023.104289.

Hendrickx, G.G., Fivash, G.S., Gerristma, A., Geraeds, M.E.G., Pearson, S.G., 2025. Socio-ecological evaluation of estuary-scale interventions. Ecol. Eng. (in prep).

Hendrickx, G.G., Kranenburg, W.M., Antolínez, J.A.A., Huismans, Y., Aarninkhof, S.G.J., Herman, P.M.J., 2023b. Sensitivity of salt intrusion to estuary-scale changes: A systematic modelling study towards nature-based mitigation measures. Estuar. Coast. Shelf Sci. 295, 108564. http://dx.doi.org/10.1016/j.ecss.2023.108564.

Hendrickx, G.G., Manuel, L.A., Pearson, S.G., Aarninkhof, S.G.J., Meselhe, E.A., 2024. An earthen sill as a measure to mitigate salt intrusion in estuaries. Estuaries Coasts 47 (5), 1199–1208. http://dx.doi.org/10.1007/s12237-024-01359-2.

Hesen, P., 2021. Projectbeslissing KWA+: Maatregelenpakket C. Technical Report, Hoogheemraadschap De Stichtse Rijnlanden en Hoogheemraadschap van Rijnland, URL: https://hdsr.bestuurlijkeinformatie.nl/Document/View/8300812c-466f-4d3a-a600-485ff39274ed.

HydroLogic, 2015. Verzilting door verdieping Nieuwe Waterweg en Botlek. Technical Report december, HydroLogic, Amersfoort, the Netherlands.

HydroLogic, 2018. Vervolgonderzoek Kosten En Effecten Permanente Oostelijke Zoetwateraanvoer Voor West-Nederland. Technical Report, HydroLogic, Amersfoort, the Netherlands, URL: https://www.stroming.nl/nl/overzicht/laagwaterbeheer-laag-nederland.

HydroLogic, 2019a. Optimalisatie Wateraanvoer West-Nederland. Technical Report, HydroLogic, Amersfoort, the Netherlands, URL: https://www.stroming.nl/nl/overzicht/laagwaterbeheer-laag-nederland.

HydroLogic, 2019b. Rijn-Maasmonding: Slim Watermanagement Redeneerlijn Watertekort. Technical Report, HydroLogic, Amersfoort, the Netherlands, URL: https://open.rijkswaterstaat.nl/open-overheid/onderzoeksrapporten/@195399/rijn-maasmonding-slim-watermanagement/.

Johnson, B.H., Boyd, M.B., Keulegan, G.H., 1987. A Mathematical Study of the Impact on Salinity Intrusion of Deepening the Lower Mississippi River Navigation Channel. Technical Report, Hydraulic Laboratory, US Army Engineer Waterways Experiment Station, Vicksburg, MS, USA, URL: https://henry.baw.de/items/bd81f0a1-ee82-4ad7-a41f-e7da39267c0e.

Jones, E.R., Bierkens, M.F.P., van Vliet, M.T.H., 2024. Current and future global water scarcity intensifies when accounting for surface water quality. Nat. Clim. Chang. 1–7. http://dx.doi.org/10.1038/s41558-024-02007-0.

Keeney, R.L., 1996. Value-focused thinking: Identifying decision opportunities and creating alternatives. European J. Oper. Res. 92 (3), 537–549. http://dx.doi.org/10.1016/0377-2217(96)00004-5.

Keeney, R.L., Raiffa, H., 1993. Decisions with multiple objectives. Decisions with Multiple Objectives. Cambridge University Press, Cambridge, United Kingdom, p. 569. http://dx.doi.org/10.1017/cbo9781139174084.

Kind, J.M., 2014. Economically efficient flood protection standards for the Netherlands. Flood Risk Manag. 7, 103–117. http://dx.doi.org/10.1111/jfr3.12026.

Klijn, F., van Velzen, E., ter Maat, J., Hunink, J., 2012. Zoetwatervoorziening in Nederland: Aangescherpte Landelijke Knelpuntenanalyse 21e Euuw. Technical Report, Deltares, Delft, the Netherlands, URL: https://research.wur.nl/en/publications/zoetwatervoorziening-in-nederland-aangescherpte-landelijke-knelpu.

Kragt, M.E., 2013. Hydro-economic modelling in an uncertain world: Integrating costs and benefits of water quality management. Water Resour. Econ. 4, 1–21. http://dx.doi.org/10.1016/j.wre.2013.11.001.

Kranenburg, W.M., van der Kaaij, T., Nolte, A.J., 2015. Evaluatie Van Het OSR-Model Voor Zoutindringing in De Rijn-Maasmonding (II). Technical Report, Deltares, Delft, the Netherlands, URL: https://www.deltares.nl/expertise/publicaties/evaluatie-van-het-osr-model-voor-zoutindringing-in-de-rijn-maasmonding-ii.

Kranenburg, W.M., Tiessen, M.C., Blaas, M., Van Veen, N.P., 2023. Circulation, stratification and salt dispersion in a former estuary after reintroducing seawater inflow. Estuar. Coast. Shelf Sci. 282, 108221. http://dx.doi.org/10.1016/j.ecss.2023.108221.

Kumar, S., Lawrence, D.M., Dirmeyer, P.A., Sheffield, J., 2013. Less reliable water availability in the 21st century climate projections. Earth's Futur. 2 (3), 152–160. http://dx.doi.org/10.1002/2013EF000159.

Lee, J., Biemond, B., de Swart, H., Dijkstra, H.A., 2024. Increasing risks of extreme salt intrusion events across European estuaries in a warming climate. Commun. Earth Environ. 5 (1), 60. http://dx.doi.org/10.1038/s43247-024-01225-w.

Loreau, M., Mouquet, N., Gonzalez, A., 2003. Biodiversity as spatial insurance in heterogeneous landscapes. Proc. Natl. Acad. Sci. USA 100 (22), 12765–12770. http://dx.doi.org/10.1073/pnas.2235465100.

Maul, G.A., Duedall, I.W., 2019. Demography of coastal populations. In: Finkl, C.W., Makowski, C. (Eds.), Encyclopedia of Coastal Science. Springer International Publishing, pp. 692–700. http://dx.doi.org/10.1007/978-3-319-93806-6_115.

Mestdagh, S., Fang, X., Soetaert, K., Ysebaert, T., Moens, T., Van Colen, C., 2020. Seasonal variability in ecosystem functioning across estuarine gradients: The role of sediment communities and ecosystem processes. Mar. Environ. Res. 162, 105096. http://dx.doi.org/10.1016/j.marenvres.2020.105096.

Meyers, S.D., Yilmaz, Y., Luther, M.E., 2022. Some methods for addressing errors in static AIS data records. Ocean Eng. 264, 112367. http://dx.doi.org/10.1016/j.oceaneng.2022.112367.

Miettinen, K., 1998. A posteriori methods. In: Nonlinear Multiobjective Optimization. Springer, MA, pp. 77–113. http://dx.doi.org/10.1007/978-1-4615-5563-6_4.

Miller, P.W., Hiatt, M., 2024. Hydrometeorological drivers of the 2023 louisiana water crisis. Geophys. Res. Lett. 51 (10), http://dx.doi.org/10.1029/2024GL108545.

Morris, R.K., 2013. Geomorphological analogues for large estuarine engineering projects: A case study of barrages, causeways and tidal energy projects. Ocean & Coastal Management 79, 52–61. http://dx.doi.org/10.1016/j.ocecoaman.2012.05.010.

Muller, J.Z., 2021. The perils of metric fixation. Med. Teach. 43 (6), 622–624. http://dx.doi.org/10.1080/0142159X.2020.1840745.

Nguyen, V.T., Le, V.A., 2023. Fluid mud properties and nautical depth estimation: A case study in navigation channel of Duyen Hai Port, Vietnam. Ocean Eng. 284, 115163. http://dx.doi.org/10.1016/j.oceaneng.2023.115163.

Orton, P., Ralston, D., van Prooijen, B., Secor, D., Ganju, N., Chen, Z., Fernald, S., Brooks, B., Marcell, K., 2023. Increased utilization of storm surge barriers: A research agenda on estuary impacts. Earth's Futur. 11, http://dx.doi.org/10.1029/2022EF002991.

Park, S.W., Lee, M.K., Park, Y.S., 2020. Analysis and improvement of communications in port areas using the queuing theory. J. Navig. 73 (4), 912–931. http://dx.doi.org/10.1017/S0373463320000041.

Pearson, S., Windupranata, W., Pranowo, S.W., Putri, A., Ma, Y., Vila-Concejo, A., Fernández, E., Mébdez, G., Banks, J., Knights, A.M., Firth, L.B., Bollard Breen, B., Jarvis, R., Aguirre, J.D., Chen, S., Howard Smith, A.N., Steinberg, P., Chatzinikolaou, E., Arvanitidis, C., 2016. Conflicts in some of the world harbours: what needs to happen next? Marit. Stud. 15 (10), http://dx.doi.org/10.1186/s40152-016-0049-x.

Pinto, R., de Jonge, V.N., Neto, J.M., Domingos, T., Marques, J.C., Patrício, J., 2013. Towards a DPSIR driven integration of ecological value, water uses and ecosystem services for estuarine systems. Ocean & Coastal Management 72, 64–97. http://dx.doi.org/10.1016/j.ocecoaman.2011.06.016.

Pont, D., Day, J.W., Hensel, P., Franquet, E., Torre, F., Rioual, P., Ibànez, C., Coulet, E., 2002. Response scenarios for the deltaic plain of the Rhône in the face of an acceleration in the rate of sea-level rise with special attention to Salicornia-type environments. Estuaries 25 (3), 337–358. http://dx.doi.org/10.1007/BF02695978.

Port of Rotterdam, 2024. Throughput Port of Rotterdam. Technical Report, Port of Rotterdam, Rotterdam, the Netherlands, URL: https://www.portofrotterdam.com/en/news-and-press-releases/cargo-throughput-port-rotterdam-slightly-decreased-2024).

Pourteimouri, P., den Haan, R.J., Kwadijk, J., van der Voort, M., 2024. Developing an integrated assessment model for salt intrusion mitigation measures in delta systems. In: Niesten, I., Tahsin, N., van Grootheest, D., Barneveld, H., Waldschläger, K., Hoitink, T. (Eds.), NCR Days. Netherlands Centre for River Studies, Wageningen, the Netherlands, pp. 113–114, URL: https://research.utwente.nl/en/publications/developing-an-integrated-assessment-model-for-salt-intrusion-miti.

Ralston, D.K., Geyer, W.R., 2019. Response to channel deepening of the salinity intrusion, estuarine circulation, and stratification in an Urbanized Estuary. J. Geophys. Res.: Ocean. 124 (7), 4784–4802. http://dx.doi.org/10.1029/2019JC015006.

Reeze, B., de la Haye, M.A.A., van der Jagt, H.A., Verweij, G.L., 2022. Vervolgrapportage Ecologische Toestand Haringvliet En Voordelta 'Lerend Implementeren Kierbesluit' 2020. Technical Report, Bureau Waardenburg, Culemborg, the Netherlands, URL: https://edepot.wur.nl/660266.

Rijkswaterstaat, 2019. Water Management in the Netherlands. Technical Report, Rijkswaterstaat, URL: https://www.helpdeskwater.nl/publish/pages/165190/rij_8475_watermanagement_en_dv_1.pdf.

Rijkswaterstaat, 2023. Watermanagementcentrum Nederland: Jaaroverzicht 2022. Technical Report, Watermanagementcentrum Nederland, Lelystad, the Netherlands, URL: https://iplo.nl/publish/pages/199528/jaarverslag-wmcn-2022t.pdf.

Sperna Weiland, F., Hegnauer, M., Bouaziz, L., Beersma, J., 2015. Implications of the KNMI'14 Climate Scenarios for the Discharge of the Rhine and Meuse. Technical Report, Deltares, Delft, the Netherlands, URL: https://publications.deltares.nl/1220042_000.pdf.

Tangelder, M., Winter, E., Ysebaert, T., 2017. Ecologie Van Zoet-Zout Overgangen in Deltagebieden: literatuurstudie En Beoordeling Van Een Scenario in Het Volkerak-Zoommeer. Technical Report, Wageningen University & Research, Wageningen, the Netherlands, http://dx.doi.org/10.18174/436428.

Temmerman, S., Meire, P., Bouma, T.J., Herman, P.M.J., Ysebaert, T., de Vriend, H.J., 2013. Ecosystem-based coastal defence in the face of global change. Nature 504 (7478), 79–83. http://dx.doi.org/10.1038/nature12859.

Tönis, I.E., Stam, J.M.T., van de Graaf, J., 2002. Morphological changes of the haringvliet estuary after closure in 1970. Coast. Eng. 44 (3), 191–203. http://dx.doi.org/10.1016/S0378-3839(01)00026-6.

Toreti, A., Bavera, D., Acosta Navarro, J., Cammalleri, C., de Jager, A., Di Ciollo, C., Hrast Essenfelder, A., Maetens, W., Masante, D., Magni, D., Mazzeschi, M., Spinoni, J., 2022. Drought in Europe August 2022. Technical Report, Publications Office of the European Union, Luxembourg, http://dx.doi.org/10.2760/264241.

Toreti, A., Belward, A., Perez-Dominguez, I., Naumann, G., Luterbacher, J., Cronie, O., Seguini, L., Manfron, G., Lopez-Lozano, R., Baruth, B., van den Berg, M., Dentener, F., Ceglar, A., Chatzopoulos, T., Zampieri, M., 2019. The exceptional 2018 European water seesaw calls for action on adaptation. Earth's Futur. 7 (6), 652–663. http://dx.doi.org/10.1029/2019EF001170.

Tulp, I., Bolle, L.J., Rijnsdorp, A.D., 2008. Signals from the shallows: In search of common patterns in long-term trends in Dutch estuarine and coastal fish. J. Sea Res. 60 (1–2), 54–73. http://dx.doi.org/10.1016/j.seares.2008.04.004.

Ueda, T., Ogawa, M., Sugimura, Y., Kawasaki, T., Matsuda, T., 2025. Predicting the maximum size of container vessels in the future. Res. Transp. Bus. Manag. 61 (101382), http://dx.doi.org/10.1016/j.rtbm.2025.101382.

Unie van Waterschappen, 2022. WAVES. URL: https://live-waves.databank.nl/.

van Alphen, J., Haasnoot, M., Diermanse, F., 2022. Uncertain accelerated sea-level rise, potential consequences, and adaptive strategies in the Netherlands. Water 14 (10), 1527. http://dx.doi.org/10.3390/w14101527.

van den Brink, M., Huismans, Y., Blaas, M., Zwolsman, G., 2019. Climate change induced salinization of drinking water inlets along a tidal branch of the Rhine River: Impact assessment and an adaptive strategy for water resources management. Climate 7 (4), 49. http://dx.doi.org/10.3390/cli7040049.

van der Baan, J., van der Heijden, S., van Reen, M., 2023. Systeemanalyses Zoetwater Regio Amsterdam-Rijnkanaal - Noordzeekanaal. Technical Report, Arcadis/Hydrologic, URL: https://www.rijksoverheid.nl/documenten/rapporten/2023/01/19/systeemanalyses-zoetwater-regio-amsterdam-rijnkanaal-noordzeekanaal.

van der Heijden, S., Koomen, A., Menke, M., 2024. Mogelijke varianten Klimaatbestendige Zoetwatervoorziening Hoofdwatersysteem. Technical Report, Arcadis, Amersfoort, the Netherlands, URL: https://open.rijkswaterstaat.nl/zoeken/@269580/mogelijke-varianten-klimaatbestendige/.

van Koningsveld, M., den Uijl, J.A.W., 2019. OpenTNSim (version 0.0.1). http://dx.doi.org/10.5281/zenodo.3341517, Software.

van Koningsveld, M., Verheij, H.J., Taneja, P., de Vriend, H., 2023. Ports and waterways – navigating the changing world. In: Ports and Waterways – Navigating the Changing World. TU Delft Open, Delft, the Netherlands, http://dx.doi.org/10.5074/T.2021.004.

Veerapaga, N., Shintani, T., Azhikodan, G., Yokoyama, K., 2020. Study on salinity intrusion and mixing types in a conceptual estuary using 3-D hydrodynamic simulation: Effects of length, width, depth, and bathymetry. In: Nguyen, K., Guillou, S., Gourbesville, P., Thiébot, J. (Eds.), Estuaries and Coastal Zones in Times of Global Change. Springer Singapore, Singapore, pp. 13–30. http://dx.doi.org/10.1007/978-981-15-2081-5_2.

Vinke, F., van Koningsveld, M., van Dorsser, C., Baart, F., van Gelder, P., Vellinga, T., 2022. Cascading effects of sustained low water on inland shipping. Clim. Risk Manag. 35, 100400. http://dx.doi.org/10.1016/j.crm.2022.100400.

Vinke, F., Turpijn, B., van Gelder, P., van Koningsveld, M., 2024. Inland shipping response to discharge extremes – A 10 years case study of the Rhine. Clim. Risk Manag. 43, 100578. http://dx.doi.org/10.1016/j.crm.2023.100578.

Vörösmarty, C.J., Green, P., Salisbury, J., Lammers, R.B., 2000. Global water resources: Vulnerability from climate change and population growth. Science 289 (5477), 284–288. http://dx.doi.org/10.1126/science.289.5477.284.

Wada, Y., van Beek, L.P.H., Viviroli, D., Dürr, H.H., Weingartner, R., Bierkens, M.F.P., 2011. Global monthly water stress: 2. Water demand and severity of water stress. Water Resour. Res. 47 (7), http://dx.doi.org/10.1029/2010WR009792.

Wannasin, C., Biemond, B., Wullems, B., Blokhuijsen, T., Tiessen, M., Baart, F., Kwadijk, J., 2024. Virtual Delta: a digital twin for real-time forecasting and management of saltwater intrusion in the rhine-meuse delta. In: EGU. Copernicus Meetings, Vienna, Austria, p. 12982. http://dx.doi.org/10.5194/EGUSPHERE-EGU24-12982.

Wegman, T.M., Pietrzak, J.D., Horner-Devine, A.R., Dijkstra, H.A., Ralston, D.K., 2025. Forcing mechanisms of salt intrusion in a low-lying river delta during a prolonged drought. J. Geophys. Res.: Ocean. ((submitted for publication)).

van Wesenbeeck, B.K., Mulder, J.P.M., Marchand, M., Reed, D.J., de Vries, M.B., de Vriend, H.J., Herman, P.M.J., 2014. Damming deltas: A practice of the past? Towards nature-based flood defenses. Estuar. Coast. Shelf Sci. 140, 1–6. http://dx.doi.org/10.1016/j.ecss.2013.12.031.

van der Wiel, K., Lenderink, G., de Vries, H., 2021. Physical storylines of future European drought events like 2018 based on ensemble climate modelling. Weather. Clim. Extrem. 33, 100350. http://dx.doi.org/10.1016/j.wace.2021.100350.

van der Wijk, R., 2016. Afvoerverdeling En Beschikbare Metingen Rijnmaasmonding. Technical Report, Deltares, Delft, the Netherlands, URL: https://www.deltares.nl/expertise/publicaties/afvoerverdeling-en-beschikbare-metingen-rijnmaasmonding.

van der Wijk, R., 2020. Draaiboek Serious Game Rijn-Maasmonding. Technical Report, Deltares, Delft, the Netherlands.

Yang, Z., Sobocinski, K.L., Heatwole, D., Khangaonkar, T., Thom, R., Fuller, R., 2010. Hydrodynamic and ecological assessment of nearshore restoration: A modeling study. Ecol. Model. 221 (7), 1043–1053. http://dx.doi.org/10.1016/j.ecolmodel.2009.07.011.

Ysebaert, T., Herman, P.M.J., Meire, P., Craeymeersch, J., Verbeek, H., Heip, C.H.R., 2003. Large-scale spatial patterns in estuaries: Estuarine macrobenthic communities in the Schelde estuary, NW Europe. Estuar. Coast. Shelf Sci. 57 (1–2), 335–355. http://dx.doi.org/10.1016/S0272-7714(02)00359-1.

Yuan, R., Zhu, J., 2015. The effects of dredging on tidal range and saltwater intrusion in the Pearl River Estuary. J. Coast. Res. 316 (6), 1357–1362. http://dx.doi.org/10.2112/JCOASTRES-D-14-00224.1.

van Zaanen, I., Ottink, R., Sibma, M., 2022. Droogteseizoen 2022. Technical Report, Infram, Maarn, the Netherlands, URL: https://open.rijkswaterstaat.nl/@253589/droogteseizoen-2022-terugblik-wmcn-lcw/.

Zhao, T., Xiong, S., Tian, Y., Wu, Y., Li, B., Chen, X., 2024. Compound dry and hot events over major river basins of the world from 1921 to 2020. Weather. Clim. Extrem. 44, 100679. http://dx.doi.org/10.1016/j.wace.2024.100679.

Zilio, M.I., London, S., Perillo, G.M., Cintia Piccolo, M., 2013. The social cost of dredging: The Bahia Blanca Estuary case. Ocean. Coast. Manag. 71, 195–202. http://dx.doi.org/10.1016/j.ocecoaman.2012.09.008.